Journal Name

ARTICLE

Mechanistic Studies of 1,3-Dipolar Cycloadditions of Bicyclic Thioisomünchnones with Alkenes. A Computational Rationale Focused on Donor-Acceptor Interactions

Received 00th January 20xx,
Accepted 00th January 20xx

DOI: 10.1039/x0xx00000x

www.rsc.org/

Juan García de la Concepción,[a,*] Martín Ávalos,[a,] Pedro Cintas,[a,*] José L. Jiménez,[a] and Mark E. Light[b]

This paper describes a mechanistic study, in the interplay of experiment and theory, on the cycloadditions of a bicyclic mesoionic 1,3-dipole versus a series of representative symmetrical (1-phenyl-1*H*-pyrrole-2,5-dione and dimethyl maleate) and asymmetrical [(*E*)-(2-nitrovinyl)benzene, acrylonitrile, and but-3-en-2-one] olefinic dipolarophiles. These results allow a comparative analysis with monocyclic dipoles and open further avenues to structurally diversified heteroatom-rich rings. The unichiral version of the bicyclic dipole leads to adducts containing up to five chiral centers, whose formation proceeds with high levels of facial stereoinduction in reactions involving bulky dipolarophiles. The second and largest part of this study provides a theoretical interrogation on the pericyclic mechanism with DFT-methods [M06-2X/6-311G++(d,p)]. In order to extract even subtle mechanistic details at the bottom, we have also explored charge transfers between reaction partners using an NBO analysis, which satisfactorily justifies the stereochemical outcome.

Introduction

1,3-Dipolar cycloadditions represent an indispensable synthetic tool to construct five- and six-membered rings in an expeditious fashion and often with high levels of regio- and stereoselection.[1] This assembly exploits a wide range of unsaturated dipolarophiles in conjunction with some reactive dipoles, which usually exhibit a remarkable orthogonality to other functional groups. As a result, this family of pericyclic reactions has found interesting applications in biological studies[2,3] and materials design.[4]

The search for reactive, yet functionalized, dipoles capable of building-up complex structures with stereocontrol is still a must. Mesoionics, once considered exotic ionic structures and showing significant electron delocalization, are always an appropriate choice given their versatility and facile supply of polyheteroatomic arrangements in one-pot condensations.[5,6] The use of mesoionics is however limited by the steps required to obtain such heterocycles and the intrinsic stability of their structure, which often hamper high-yielding synthesis of the target products.[7]

For many years we have been interested in the design of mesoionic dipoles and their utility in heterocycle synthesis with a focus on stereocontrolled strategies.[8] Explorations with a modified 1,3-thiazolium-4-olate (usually nicknamed thioisomünchnone) bearing a dialkylamino group constituted a watershed as the latter exerted a pivotal stereoelectronic effect enabling the preparation of hitherto unknown heterocycles by conventional dipolar cycloadditions.[6b]

While most thioisomünchnones undergo dipolar cycloadditions with alkenes to provide stable bridged cycloadducts, which eventually fragment into pyrid-2-ones by a stepwise elimination of hydrogen sulfide, other thioisomünchnones give rise to dihydrothiophenes when reacted with β-nitrostyrenes.[9,10] Although the structural diversity in heterocyclic build-up represents a plus in mesoionics-based cycloadditions, an additional advantage of these heterocyclic dipoles is the simplified assembly of multiple fused rings, present in natural compounds and drugs, as the resulting cycloadducts might be prevented from subsequent ring opening. A conformationally-restricted mesoionic dipole as starting material would enable such decorations so long as little or no chemical evolution takes place subsequently. In recent studies, we have reported the preparation and 1,3-dipolar reactivity against substituted acetylenes of 2-phenyl-5,6-dihydrothiazolo[2,3-*b*]thiazol-4-ium-3-olate (**1**),[11] and an enantiomerically pure version (**2**), easily generated from a chiral amino alcohol,[12] which afford pyridin-2-one derivatives. We describe here the extension of their reactivity toward five well-established dipolarophiles (**3**-**7**). Prompted by the potential significance of these synthetic pursuits, our quantum calculations aimed at elucidating the reaction pathways and energy landscape now goes down to dissecting the electron distribution and orbital contribution at the saddle points, which allows a more precise rationale of the mechanism and interpretation of orbital control in dipolar cycloadditions.

[a] *Departamento de Química Orgánica e Inorgánica. Facultad de Ciencias-UEX. IACYS-Unidad de Química Verde y Desarrollo Sostenible. E-06006 Badajoz (Spain). E-mail: jugarco@unex.es. Fax: (+34) 924-271-149*
[b] *Department of Chemistry. University of Southampton. Southampton SO17 1BJ, U.K.*

† Electronic Supplementary Information (ESI) available: X-ray diffraction analysis, copies of NMR spectra of all synthetic products and cartesian coordinates for all optimized geometries. See DOI: 10.1039/x0xx00000x

Results and Discussion

Synthesis and Reactivity. The dipolar reactivity of 2-phenyl-5,6-dihydrothiazolo[2,3-*b*]thiazol-4-ium-3-olate (**1**) against symmetrically-substituted [1-phenyl-1*H*-pyrrole-2,5-dione (**3**) and dimethyl maleate (**4**)] and asymmetrically-substituted [(*E*)-(2-nitrovinyl)benzene (**5**), acrylonitrile (**6**), and but-3-en-2-one (**7**)] olefinic dipolarophiles (Figure 1) has been thoroughly investigated, leading to 1:1-cycloadducts that readily incorporate a polyheteroatomic core. Some reactions involving asymmetrical dipolarophiles (*vide infra*) have proven to be highly stereoselective and completely regioselective.

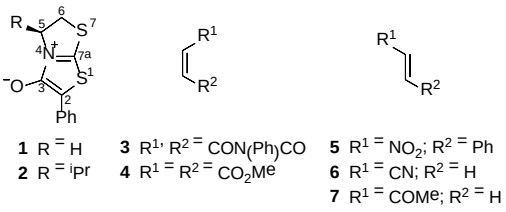

Figure 1. Structures of thioisomünchnones **1** and **2** and the set of dipolarophiles employed in this work (**3**-**7**).

The reaction of **1** and **3**, conducted in CH_2Cl_2 solution at room temperature, afforded after 24 h a mixture of the 6,8-diphenyldihydro-2*H*-6,9*b*-epithiopyrrolo[3,4-*c*]thiazolo[3,2-*a*]pyridine-5,7,9(3*H*,8*H*,9a*H*)-triones **8** and **9**, which were stable enough to be purified and isolated by crystallization in moderate yields (43% and 28%, respectively). These adducts could not be separated, however, when the reaction was carried out in toluene at reflux, as the latter evolved into a complex mixture. As we shall see later, the formation under such conditions of a fluorescent product, detected by TLC analysis, is noteworthy.

Crystals of cycloadducts **8** and **9**, suitable for X-ray diffraction analysis, could be obtained by recrystallization and slow evaporation, and their unequivocal structures are shown in Figure 2.

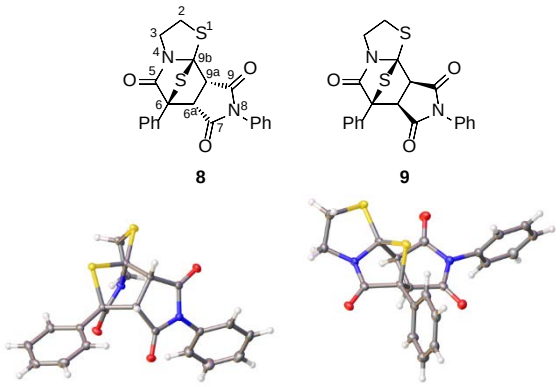

Figure 2. Structures **8** and **9** and its solid-state structures (X-ray diffractometry). Ellipsoids are shown at 50% probability.

^{1}H and ^{13}C NMR analysis are consistent with such structures and some signals possess also diagnostic value, thereby aiding the elucidation and structural correlations in these polycyclic system. The *exo* H-6a and H-9a protons of **8** show downfield shifts (4.55 and 4.30 ppm, respectively) relative to the corresponding *endo*-hydrogens of **9** (4.30 and 4.08 ppm, respectively). Moreover, the coupling constant $J_{6a,9a}$ (8.5 Hz for **8** and 7.0 Hz for **9**) allows a valuable inspection of the stereochemical course (*vide infra*).

As mentioned previously, a mixture of cycloadducts **8** and **9** heated in refluxing toluene in the presence of silica gel as catalyst afforded a fluorescent *tricyclic* pyrid-2-one (**10**). This substance could further be purified by crystallization and isolated in 54% yield.

By refluxing in toluene a mixture of **1** and **4** for 4 h, which was subsequently cooled to room temperature, the *exo* cycloadduct dimethyl 5-oxo-6-phenylhexahydro-6,8a-epithiothiazolo[3,2-*a*]pyridine-7,8-dicarboxylate (**11**) crystallized spontaneously (71% yield). Its structure was unambiguously determined by X-ray diffraction analysis (Figure 3). In contrast, the minor *endo* cycloadduct **12** could not be isolated. The *endo* H-7 and H-8 protons of **11** appeared as two doublets at 4.11 and 3.74 ppm ($J_{7,8}$ 9.0 Hz).

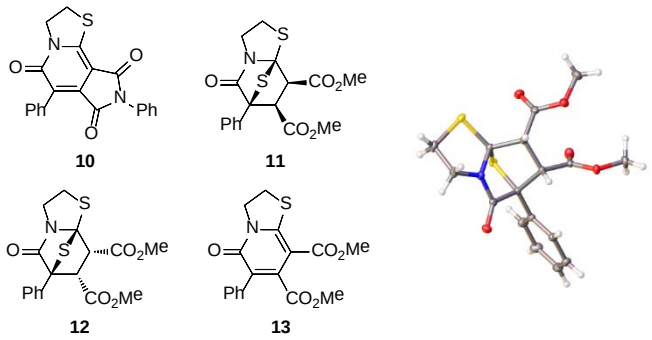

Figure 3. Chemical structures of **10**-**13** and crystal structure of cycloadduct **11** depicted at 50% ellipsoid probability.

When cycloadduct **11** was heated at reflux in toluene for prolonged time (80 h) with silica gel as heterogeneous catalyst, a new fluorescent compound appeared in the reaction mixture, whose structure was tentatively assigned to dimethyl 5-oxo-6-phenyl-3,5-dihydro-2*H*-thiazolo[3,2-*a*]pyridine-7,8-dicarboxylate (**13**). Unfortunately, all attempts to get this substance in pure form failed.

Although the cycloaddition of **1** with non-symmetrical alkenes (**5**-**7**) would afford four cycloadducts in every case, the reaction of **1** and **5** (1:1.5 molar ratio) in CH_2Cl_2 at room temperature for 72 h selectively gave rise to 8-nitro-6,7-diphenyltetrahydro-6,8a-epithiothiazolo[3,2-*a*]pyridin-5(6*H*)-one (**14**) in 63% yield, whose structure could be verified by single crystal X-ray diffraction (Figure 4). The *endo* H-7 and *exo* H-8 protons of **14**, which resonated as two doublets ($J_{7,8}$ 4.5 Hz) at 4.54 and 5.78 ppm, respectively, correlated well (HSQC experiment) with the corresponding peaks of C-7 (57.0 ppm) and C-8 (97.8 ppm) carbon atoms, while the C-6 and C-8a

bridgehead carbon atoms resonated at 77.3 and 86.2 ppm, respectively.

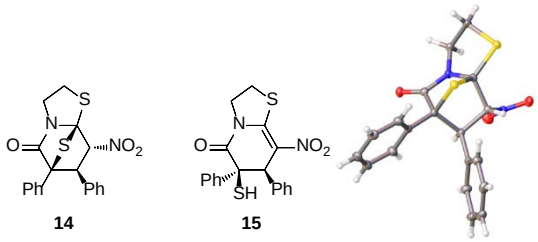

14 **15**

Figure 4. Chemical structures of **14** and **15** and crystal structure of cycloadduct **14** shown at 50% ellipsoid probability.

A solution of **14** in CH_2Cl_2 kept at room temperature for several days led to the formation of 6-mercapto-8-nitro-6,7-diphenyl-6,7-dihydro-2*H*-thiazolo[3,2-*a*]pyridin-5(3*H*)-one (**15**) (52% yield). This conversion was essentially complete within 19 h by refluxing a solution of **14** in CH_2Cl_2 containing silica gel. Two singlet signals at 2.33 ppm and 5.33 ppm, attributale to the SH and H-7 protons respectively, along with chemical shifts characteristic of C-6, C-7, C-8, and C-8a carbon atoms (60.0, 50.5, 126,4, and 154,4 ppm, respectively) confirmed the structure of **15** (see ESI).

The cycloaddition of **1** with acrylonitrile (**6**) was carried out at room temperature using the dipolarophile itself as solvent. After 24 h the mixture was quenched and two major cycloadducts could be isolated by column chromatography in low yield (18 and 20% for **16** and **17** respectively). Suitable crystals for X-ray diffraction analysis allowed us to identify them as 5-oxo-6-phenylhexahydro-6,8*a*-epithiothiazolo[3,2-*a*]pyridine-8-carbonitriles **16** and **17** (Figure 5).

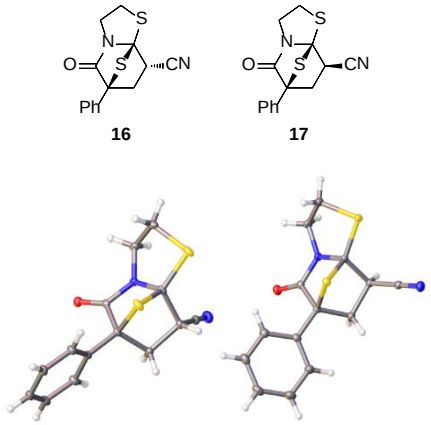

16 **17**

Figure 5. Chemical formulas of **16** and **17** accompanied by their crystal structures. Ellipsoids are shown at 50% probability.

The more relevant difference observed in the ^{1}H NMR spectra of **16** and **17** correspond to the chemical shifts of their H-8 protons that appeared as double doublets at 3.96 ppm (**16**) and 3.56 pm (**17**). Also, the coupling constants measured in such signals (J = 4.0 and 10.0 Hz for **16** and J = 3.5 Hz and 8.0 Hz for **17**) have diagnostic value.

On refluxing for 30 min a mixture containing **1** and but-3-en-2-one (**7**), compound **18**, 8-acetyl-6-[(3-oxobutyl)thio]-6-phenyl-6,7-dihydro-2*H*-thiazolo[3,2-*a*]pyridin-5(3*H*)-one, could be isolated in 32% yield. Again, adequate crystals for X-ray diffractometry revealed the unambiguous structure shown in Figure 6. The formation of **18** can be judiciously rationalized in terms of a conjugate addition involving the non-isolated thiol **19** plus an additional molecule of but-3-en-2-one.

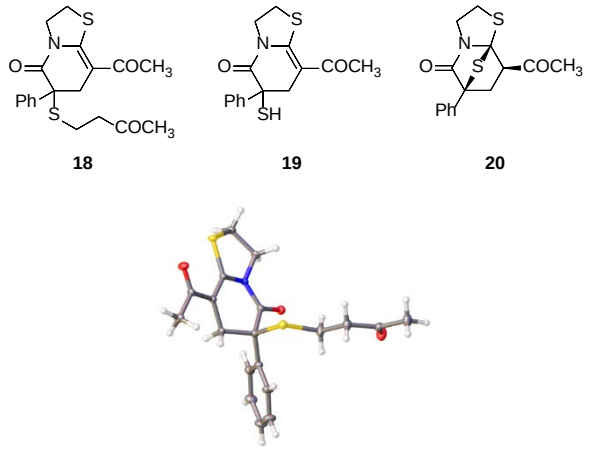

18 **19** **20**

Figure 6. Chemical formulas of **18**-**20** and solid-state structure of compound **18**. Thermal ellipsoids are shown at 50% probability.

The *exo* cycloadduct **20** could also be isolated from the reaction mixture by column chromatography in 22% yield. Its ^{1}H NMR spectrum indicated that the H-8 proton resonates at lower field (4.99 ppm) than the corresponding H-8 protons of **16** and **17**. Moreover, its coupling constants are smaller than those measured in the proton spectrum of **17** (J = 2.5 Hz and 6.5 Hz).

In a recent computational study we have shown that the size of the dipolarophile is a key feature in facial stereocontrol as inferred from an isopropyl group attached to *unichiral*[13] thioisomünchnone **2**.[12] To prove this concept further, this work now enlarges the scope of cycloadditions of **2** with other bulky dipolarophiles like **3** and **5**. The cycloaddition of **2** with 1-phenyl-1*H*-pyrrole-2,5-dione (**3**) was performed under the same conditions described above for the reaction of **1** and **3**. Inspection of the reaction mixture by TLC analysis showed the formation of several products, although only the unichiral *exo*-cycloadducts **21** and **22** could be isolated by fractional crystallization in 72% and 15% yield, respectively. Once again, single-crystal X-ray analysis proved to be instrumental in structural elucidation and Figure 7 shows the solid-state structure of (3*S*,6*R*,6*aR*,9*aS*,9*bR*)-3-isopropyl-6,8-diphenyldihydro-2*H*-6,9*b*-epithiopyrrolo[3,4-*c*]thiazolo[3,2-*a*]pyridine-5,7,9(3H,8H,9*a*H)-trione (**22**). Its ^{1}H and ^{13}C NMR data were quite similar to those of **21**. Thus, ^{1}H NMR spectra of **21** and **22** showed doublet signals at ~4.1 ppm (H-6a) and ~3.8 ppm (H-9a) with coupling constants ($J_{6a,9a}$ = 7.0 Hz) identical to those found in the ^{1}H NMR spectrum of **9**.

As described before for the transformation of **11** into **13**, cycloadducts **21** and **22** were converted in refluxing toluene containing silica gel into enantiopure (*S*)-3-isopropyl-6,8-diphenyl-2,3-dihydropyrrolo[3,4-*c*]thiazolo[3,2-*a*]pyridine-5,7,9(8*H*)-trione (**23**) in 37 % yield.

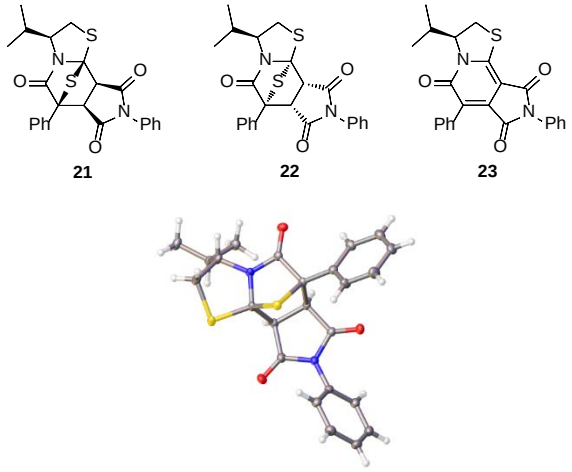

Figure 7. Chemical formulas of **21**-**23** and crystal structure of **22** with thermal ellipsoids at 50% probability.

On the other hand, the chiral dipole **2** reacted with (*E*)-(2-nitrovinyl)benzene (**5**) (1:1.1 ratio) in CH_2Cl_2 at room temperature for 30 h, to give (3*S*,6*S*,7*R*,8*R*,8*aS*)-3-isopropyl-8-nitro-6,7-diphenyltetrahydro-6,8*a*-epithiothiazolo[3,2-*a*]pyridin-5(6*H*)-one (**24**) in 78% yield. However, starting from a 1:1.5 (dipole:dipolarophile) ratio a mixture of **24** (33%) and the thioether derivative **25** (22%) was isolated after 48 h. The origin of the latter might reasonably be interpreted by spontaneous breakage of the C_{8a}-S bond in **24** followed by nucleophilic addition of the SH group of **26** on the *Si* face of an extra molecule of **5**, as discussed above for the reaction of **1** with but-3-en-2-one (**7**). Moreover, the structure of **25** was determined by X-ray diffraction analysis (Figure 8).

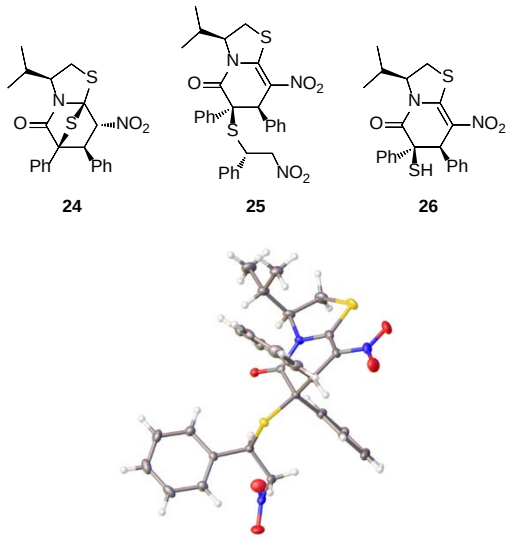

Figure 8. Chemical structures of **24**-**26** and solid-state crystal structure of **25** with thermal ellipsoids depicted at 50% probability.

In order to demonstrate unequivocally that cycloadduct **24** arises from the reaction of **2** and **5**, a solution of **24** and **5** (1:1 molar ratio) was stirred in CH_2Cl_2 for five days, leading to a complex mixture from which only the Michael-type adduct **25** could be isolated. Furthermore, a solution of **24** in refluxing CH_2Cl_2 in the presence of silica gel for 72 h did not afford thiol **26**; instead compound **25** was isolated again, thereby revealing that retro-cycloaddition of **24** releases the dipolarophile, which reacts then with **24** to give **25**. These results clearly evidence the role of bulky dipolarophiles in stereocontrolled cycloadditions with a chiral thioisomünchnone such as **2**.

Computational Analysis. Firstly, we have addressed the influence exerted by dipolarophiles on the 1,3-dipolar cycloadditions of thioisomünchnone **1** with compounds **3**-**7**. All the reactions were simulated at the M06-2X/6-311++G(d,p) level using the continuum solvation model (SMD) in the solvent employed experimentally. Accordingly, the reactions with 1-phenyl-1*H*-pyrrole-2,5-dione (**3**) and (*E*)-(2-nitrovinyl)benzene (**5**) were simulated in CH_2Cl_2, whereas the reaction with dimethyl maleate (**4**) was evaluated in toluene. Because of the reactions with acrylonitrile (**6**) and but-3-en-2-one (**7**) were carried out under neat conditions using such dipolarophiles as solvents, their role was simulated computationally by means of 2-propanol and *N*,*N*-dimethylacetamide, respectively.

The reactions of **1** with symmetrical dipolarophiles **3** and **4** are highly concerted processes that could lead to *endo* cycloadducts **8** and **12** and/or to their *exo* isomers **9** and **11**, respectively. Both *endo* and *exo* approaches of **3** to thioisomünchnone **1** are characterized by very similar energy barriers. This small energy difference clearly accounts for the experimental isolation of both diastereomers (Figure 9, left). In stark contrast, the reaction of **1** with **4** is more selective (Figure 9, right) and formation of diastereomer **11**, experimentally isolated, constitutes the most favorable process.

In order to understand the enhanced reactivity of dimethyl maleate (**4**) during its *exo* approach to dipole **1** (**TS_{11}**), we compared the main NBO (*natural bond orbital*)[14] interactions of the four saddle points **TS_8**, **TS_9**, **TS_{11}**, **TS_{12}**. Figure 10 shows the optimized geometries of such saddle points together with the two main orbital interactions for each structure. The most concerted cycloadditions were found for 1-phenyl-1*H*-pyrrole-2,5-dione (**3**), whereas the cycloadditions with dimethyl maleate are slightly more asynchronous. The donation process (from dipole to dipolarophile) in the four saddle points involves the same orbitals [LP(C2) of the dipole as donor and the π* of the dipolarophile as acceptor], where the strongest interaction corresponds to **TS_{12}** and the weakest one to **TS_{11}**. On the other hand the back-donation interactions for saddle points **TS_8**, **TS_9** and **TS_{12}** are weaker than the corresponding donation processes and involve the same orbitals as well, namely the π orbital of the dipolarophile as donor and the π*(C7a-N4) of the dipole as acceptor. The behavior is reversed in the most favored approach of dimethyl maleate (**TS_{11}**), for which the back-donation is markedly higher than the opposite interaction, where the acceptor orbital is the empty lone pair of the C-7a carbon atom [LV(C7a)].

As noted in our preceding synthetic analysis, the reaction of **1** with unsymmetrical dipolarophiles (**5**-**7**) would afford up to four cycloadducts in every case: **14** and **27**-**29** from [(*E*)-(2-nitrovinyl)benzene (**5**); **16**, **17**, **30**, and **31** from acrylonitrile (**6**); and **20** and **32**-**34** from but-3-en-2-one (**7**).

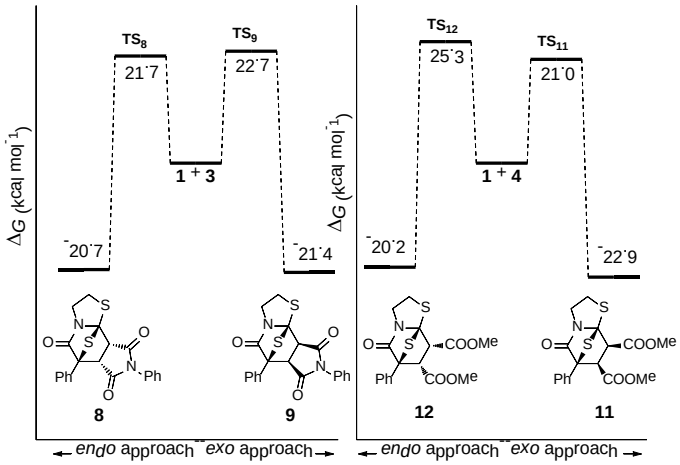

Figure 9. Relative free energy values (Δ*G*, kcal mol^{-1}) of all stationary points involved in both *endo* and *exo* approaches of **1** to **3** and **4**, calculated at the M06-2X/6-311++G(d,p) level in CH_2Cl_2 for **3** and toluene for **4** (SMD).

Figure 11 shows the free energy barriers for the four competitive approaches of **1** and **5** in CH_2Cl_2. The results indicate that cycloadducts **14** and **27** should be generated through a two-step mechanism whose first stage is the rate-limiting step. This stepwise mechanism is energetically favored with respect to the concerted mechanism leading to regioisomers **28** and **29**. The formation of **14** is kinetically favored with respect to that of **27** by ~3 kcal mol^{-1}, in good agreement with experimental results.

It is worth mentioning that factors contributing to the stabilization of zwitterionic intermediates in cycloaddition reactions, like $\mathbf{I_{14}}$ and $\mathbf{I_{27}}$ in the present work, have been discussed recently.[15] Herein, in the reaction with (*E*)-(2-nitrovinyl)benzene (**5**), the electron-withdrawing effect owing to the nitro group allows to concentrate a high electron charge that stabilizes the intermediates. The electrostatic potential maps for such two zwitterionic intermediates are shown in Figure 11, where the electron charge is highly localized on the nitro groups.

The four approaches of acrylonitrile (**6**) to thioisomünchnone **1** are concerted cycloadditions, albeit they proceed with different levels of asynchronicity (Figure 12). Thus, the formation of cycloadducts **30** and **31** occurs through more concerted pathways than the rest, although they are also energetically disfavored, pointing to a regioselective cycloaddition, in close mimicry to the cycloaddition of **1** and **5**.

The most asynchronous saddle point ($\mathbf{TS_{16}}$) is practically as stable as its diastereomer $\mathbf{TS_{17}}$ ($\Delta\Delta G^{\ddagger}$ 0.66 kcal mol^{-1}), thereby suggesting a non-diastereoselective cycloaddition as it was demonstrated experimentally.

The energy landscape of the four reaction channels of **1** with but-3-en-2-one (**7**) (Figure 13) is likewise similar to those previously described for the cycloaddition with acrylonitrile (Figure 12). The reaction is regioselective because the more asynchronous saddle points ($\mathbf{TS_{20}}$ and $\mathbf{TS_{32}}$) are more favored than their regioisomers $\mathbf{TS_{33}}$ and $\mathbf{TS_{34}}$, although the calculated $\Delta\Delta G^{\ddagger}$ [$\Delta G^{\ddagger}$($\mathbf{TS_{20}}$) - $\Delta G^{\ddagger}$($\mathbf{TS_{32}}$) < 1 kcal mol^{-1}] value would justify the lack of diastereoselectivity and the formation of both cycloadducts (**20** and **32**) in similar ratio. Moreover, this finding suggests that the formation of thioether **18** should most likely arise from the evolution of cycloadducts **20** and **32**.

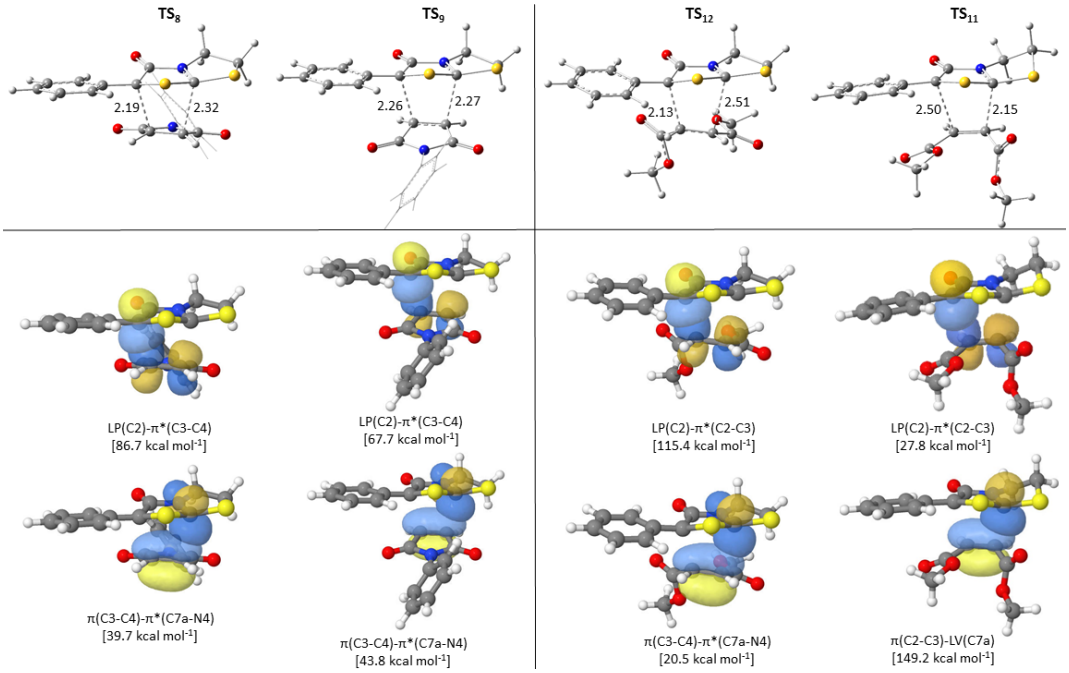

Figure 10. Optimized geometries of saddle points $\mathbf{TS_8}$, $\mathbf{TS_9}$, $\mathbf{TS_{11}}$ and $\mathbf{TS_{12}}$ at the M06-2X/6-311++G(d,p)-level in CH_2Cl_2 for **3** and in toluene for **4** (SMD). Bond distances are given in angstroms. The highest values of charge transfer found in the four saddle points are given in kcal mol^{-1}.

Journal Name

ARTICLE

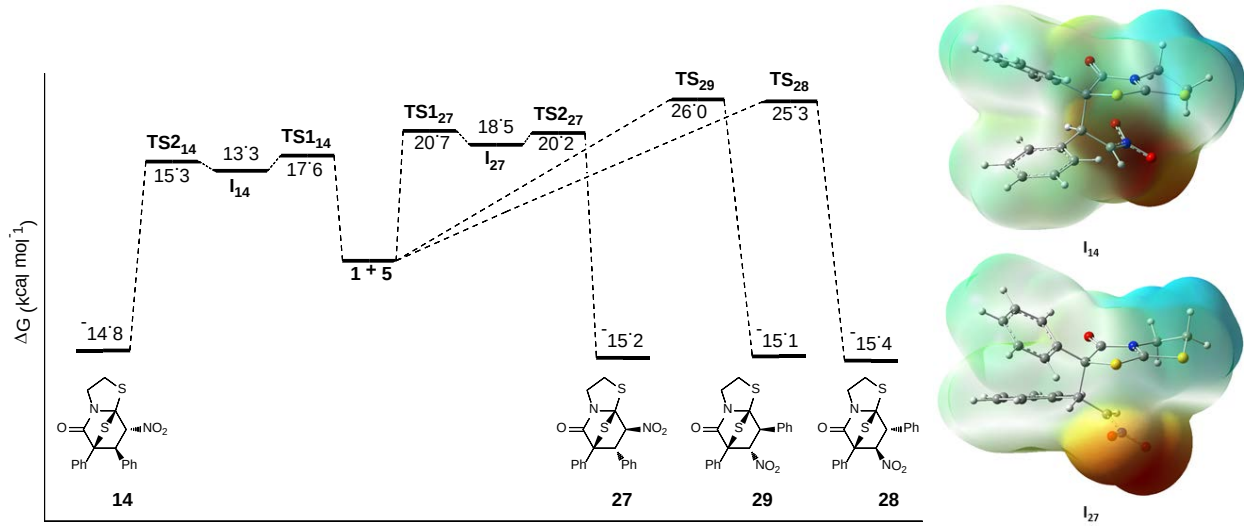

Figure 11. Left: relative free energy values (Δ*G*, kcal mol^{-1}) of all stationary points involved in the four possible reaction channels of **1** and **5** calculated at the M06-2X/6-311++G(d,p) level in CH_2Cl_2 (SMD method). Right: Electrostatic potential maps for zwitterionic intermediates $\mathbf{I_{14}}$ and $\mathbf{I_{27}}$.

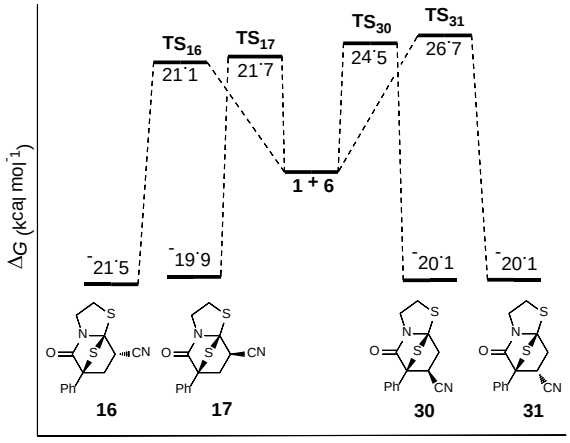

Figure 12. Relative free energy values (Δ*G*, kcal mol^{-1}) of all stationary points involved in the four possible reaction channels of **1** and **6** calculated at the M06-2X/6-311++G(d,p) level in *N*,*N*-dimethylacetamide (SMD method).

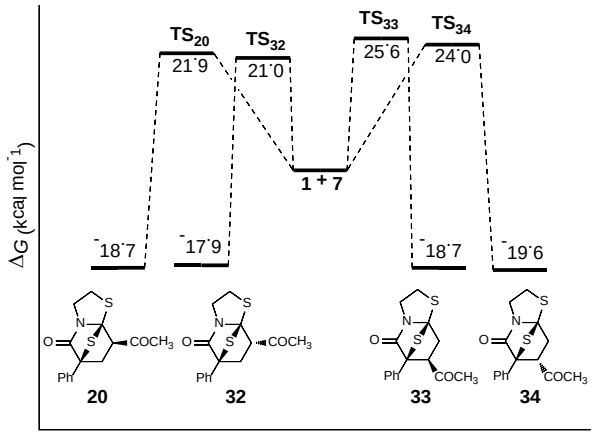

Figure 13. Relative free energy values (Δ*G*, kcal mol^{-1}) of all stationary points involved in the four possible approaches of **1** and **7** calculated at the M06-2X/6-311++G(d,p) level in 2-propanol (SMD method).

Our computational study shows that the cycloadditions of asymmetrical dipolarophiles **5**, **6** and **7** with **1** are regioselective. Moreover, the *endo* approaches for this regiochemistry are favored, albeit to a lesser extent. In order to explain this selectivity we have compared the main orbital interactions present in the saddle points $\mathbf{TS1_{14}}$, $\mathbf{TS_{16}}$ and $\mathbf{TS_{32}}$ (*endo* approaches of dipolarophiles **5**-**7** to dipole **1**) with those of the opposite regiochemistry, namely $\mathbf{TS_{29}}$, $\mathbf{TS_{31}}$ and $\mathbf{TS_{34}}$. Such geometries along with the main orbital interactions are gathered in Figures 14 and 15. The most favored approaches proceeding through $\mathbf{TS1_{14}}$, $\mathbf{TS_{16}}$ and $\mathbf{TS_{32}}$ exhibit a high charge transfer in the direction dipole-dipolarophile, whereas the corresponding back-donation is irrelevant. On the other hand, the less favored attacks occurring through $\mathbf{TS_{29}}$, $\mathbf{TS_{31}}$ and $\mathbf{TS_{34}}$ exhibit a similar behavior to those of $\mathbf{TS_{11}}$ (see Figure 10), where the back-donation dictates the charge transfer process.

Journal Name

ARTICLE

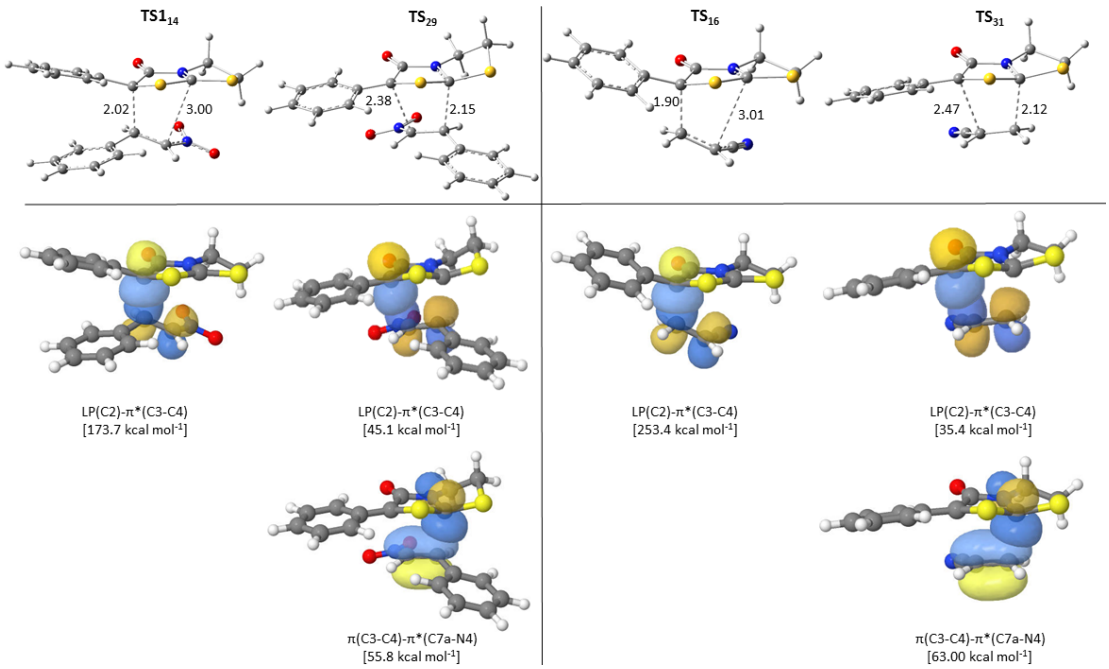

Figure 14. Optimized geometries for saddle points **TS1$_{14}$**, **TS$_{29}$**, **TS$_{16}$** and **TS$_{31}$** at the M06-2X/6-311++G(d,p)-level in CH_2Cl_2 for **5** and in *N*,*N*-dimethylacetamide for **6** (SMD). Bond distances are given in angstroms. The highest values of charge transfer found in the four saddle points are given in kcal mol^{-1}.

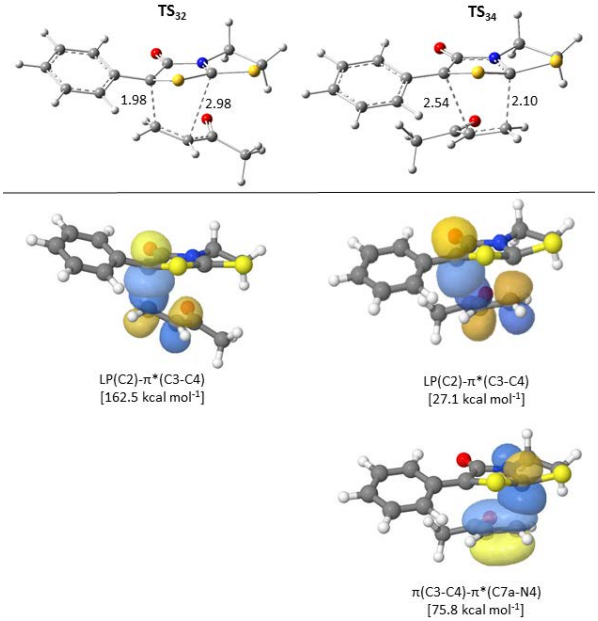

Figure 15. Optimized geometries for saddle points **TS$_{32}$** and **TS$_{34}$** at the M06-2X/6-311++G(d,p)-level in 2-propanol (SMD). Bond distances are given in angstroms. The highest values of charge transfer found in the four saddle points are given in kcal mol^{-1}.

It is worth pointing out that although the formation of **16** and **32** are concerted cycloadditions, the geometry of their saddle points **TS$_{16}$** and **TS$_{32}$** is quite similar to that of **TS1$_{14}$**, which corresponds to a stepwise process. Furthermore, the interaction energy is even higher for the cycloaddition with acrylonitrile (**TS$_{16}$**) (see Figures 14 and 15).

The IRC (intrinsic reaction coordinate) analyses for saddle points **TS$_{16}$** and **TS$_{32}$** show a caldera-like region with a pronounced depression of the energy gradient. The geometries for such structures are quite similar to **TS2$_{14}$**, which corresponds to the second saddle point of the stepwise cycloaddition of **1** with (*E*)-(2-nitrovinyl)benzene (**5**). Also the back-donation courses are similar both in orbital composition and interaction energies. In this case the lowest charge transfer was obtained in the cycloaddition with acrylonitrile (**6**) (Figure 16).

In order to assess the facial stereocontrol induced by the chiral thioisomünchnone (**2**) with the bulkiest symmetrical and asymmetrical dipolarophiles employed in this work (**3** and **5**), we have considered the formation of all the possible diastereomers, i.e. up to four in the cycloaddition with 1-phenyl-1*H*-pyrrole-2,5-dione (**21**, **22**, **35**, and **36**) and up to eight with (*E*)-(2-nitrovinyl)benzene (**24**, and **37**-**43**).

Journal Name

ARTICLE

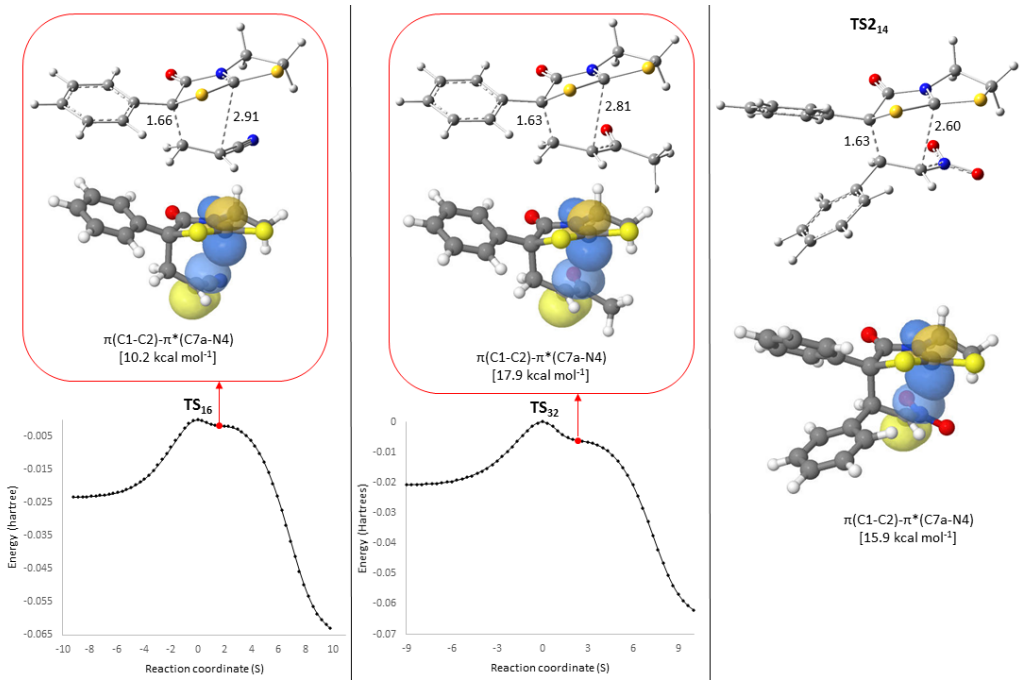

Figure 16. IRC analyses for saddle points $\mathbf{TS_{16}}$ (left) and $\mathbf{TS_{32}}$ (middle). The geometries for the lowest gradient in the caldera-type region are depicted as well together with NBO interactions during the back-donation. The optimized geometry for $\mathbf{TS2_{14}}$ at the M06-2X/6-311++G(d,p)-level in CH_2Cl_2 (SMD) and the back-donation interaction are shown on the right.

Figure 17 shows the energy barriers for the four approaches of **2** and **3**, leading to cycloadducts **21**, **22**, **35**, and **36**. The *exo*-approaches of **3** to the 2-*Re*,7a-*Re* and 2-*Si,7a-Si* faces of **2**would afford **21** and **22**, respectively, through the corresponding saddle points $\mathbf{TS_{21}}$ and $\mathbf{TS_{22}}$, whereas **35** and **36** would form, via $\mathbf{TS_{35}}$ and $\mathbf{TS_{36}}$, as a result of the *endo*-approaches of **3** to the 2-*Re*,7a-*Re* and 2-*Si,7a-Si* faces of **2**. All cycloadditions are very concerted processes and the free energies computed for $\mathbf{TS_{21}}$, $\mathbf{TS_{22}}$ and $\mathbf{TS_{35}}$ are similar to those found for $\mathbf{TS_8}$ and $\mathbf{TS_9}$ (Figure 9). The highest energy barrier corresponds to the formation of the *endo* cycloadduct **36**, where the approach of the 1*H*-pyrrole-2,5-dione ring lies near the isopropyl group ($\mathbf{TS_{36}}$) exerting a marked steric effect. However, the isopropyl group does not affect significantly the *exo* approach of **3** to the same face (2-*Si,7a-Si*) of the mesoionic ring ($\mathbf{TS_{22}}$) (*vide infra*), a fact which manifests itself in a lower energy barrier and explains the isolation of cycloadduct **22**.

A suitable algorithm for depicting, in qualitative form, the non-covalent interactions exerted by the bulky isopropyl group involves the use of the RDG (reduced density gradient)[16] function, whose 3D representation (reduced gradient multiplied by the sign of the second Hessian eigenvalue of the electron density, against the electron density) allows an eye-catching

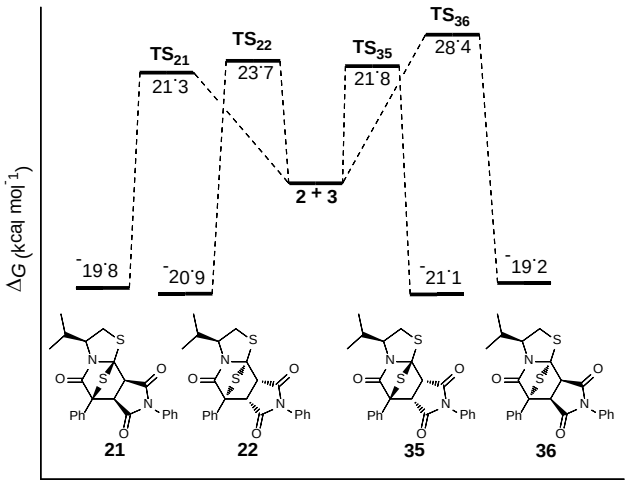

Figure 17. Relative free energy values (ΔG, kcal mol^{-1}) of all stationary points involved in the *endo* and *exo* approaches of **2** and **3** calculated at the M06-2X/6-311++G(d,p) level in CH_2Cl_2 (SMD method).

visualization of the zones where such weak interactions take place. Figure 18 shows the 3D plots of the steric and Van der Waals interactions played by the isopropyl group during the approach of **3** to thioisomünchnone **2** through the 2-*Si,7a-Si* face (**TS$_{22}$** and **TS$_{36}$**). As shown in this Figure, the 1*H*-pyrrole-2,5-dione ring lies far from the isopropyl group in the *exo* approach (**TS$_{22}$**) and the small steric repulsion is offset by the Van der Waals interaction. This situation mismatches the graphical plot for **TS$_{36}$** where the imide ring lies in close proximity to the isopropyl group and the Van der Waals interactions do not offset such a substantial steric hindrance.

The energy gaps associated to the reaction of **2** with (*E*)-(2-nitrovinyl)benzene (**5**) are collected in Figures 19 and 20. Pathways involving the approach of **5** to the 2-*Re*,7a-*Re* face of **2** (Figure 19) are more favored processes than the corresponding approaches to the 2-*Si,7a-Si* face (Figure 20), thus highlighting the facial selection exerted by the isopropyl group on a bulky dipolarophile like **5**. Notably, the reaction channels facing carbon atoms C-2 and C-7a of **2** with C-2 and C-1 of **5**, respectively, are stepwise processes whereas the reaction pathways with the opposite regiochemistry are concerted, albeit energetically less favored, processes. Stepwise cycloadditions involving the 2-*Re*,7a-*Re* face of **2** have free energy barriers similar to those shown in Figure 11, while the processes involving the 2-*Si*,7a-*Si* face are somewhat less favorable from an energy viewpoint.

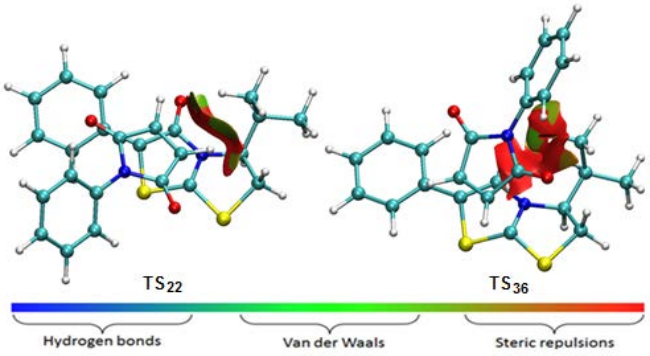

Figure 18. 3D Plots of the reduced density gradient (RDG) *versus* the electron density. Results are shown for the geometries of the transition structures **TS$_{22}$** and **TS$_{36}$** optimized at the M062X/6-311++g(d,p) level in CH_2Cl_2 (SMD).

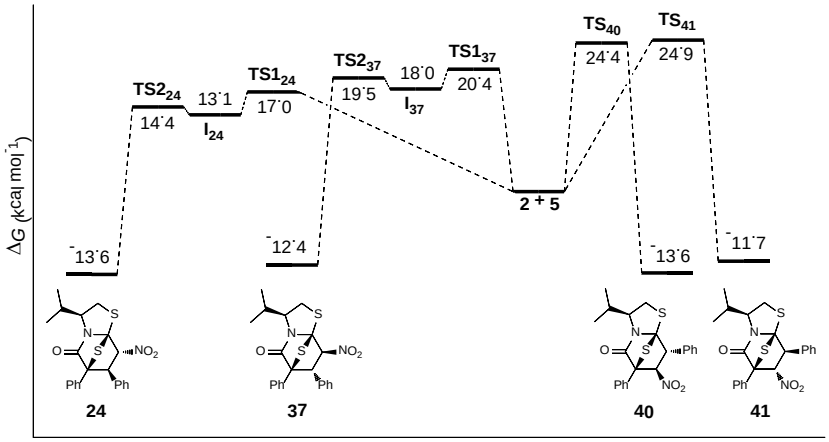

Figure 19. Relative free energy values (Δ*G*, kcal mol^{-1}) of all stationary points involved in the four approaches of **5** to the 2-*Re*,7a-*Re* face of **2** calculated at the M06-2X/6-311++G(d,p) level in CH_2Cl_2 (SMD method).

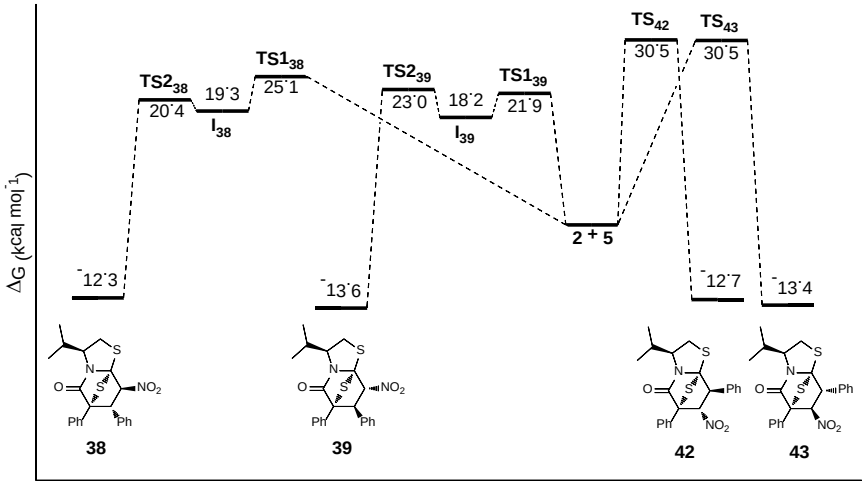

Figure 20. Relative free energy values (Δ*G*, kcal mol^{-1}) of all stationary points involved in the four approaches of **5** to the 2-*Si*,7a-*Si* face of **2** calculated at the M06-2X/6-311++G(d,p) level in CH_2Cl_2 (SMD method).

Among the cycloadditions computationally studied, the reaction of dipole **2** with (*E*)-(2-nitrovinyl)benzene appears to be the most selective process and predicts the formation of only one cycloadduct (**24**), thus corroborating the experimental results.

In order to gain further insight into the facial stereocontrol exerted by the isopropyl group of the chiral thioisomünchnone **2**, we employed the well-established distortion/interaction model to quantify the distortion energies of the reactants when they approach to both the 2-*Re*,7a-*Re* and 2-*Si*,7a-*Si* faces of **2**. The distortion/interaction or activation strain model has been found to be particularly useful to account for the experimental trends in reactivity and selectivity of some dipolar cycloadditions.[17]

Figure 21 shows the distortion energies of the dipole (in red) dipolarophiles (blue), interaction energies (green) and activation energies (black) for the saddle points calculated in the reactions of the dipole **2** with **3** (above) and **5** (below). The results obtained for the reaction with 1-phenyl-1*H*-pyrrole-2,5-dione (**3**) show that the distortion energies of the dipole mirror the free energy barriers depicted in Figure 17, where the values for the transition structures **TS$_{21}$**, **TS$_{22}$** and **TS$_{35}$** appear to be quite similar. On the other hand, the saddle point **TS$_{36}$**, which corresponds with the *endo* approach of **3** to the 2-*Si*,7a-*Si* face of **2** shows a higher distortion energy.

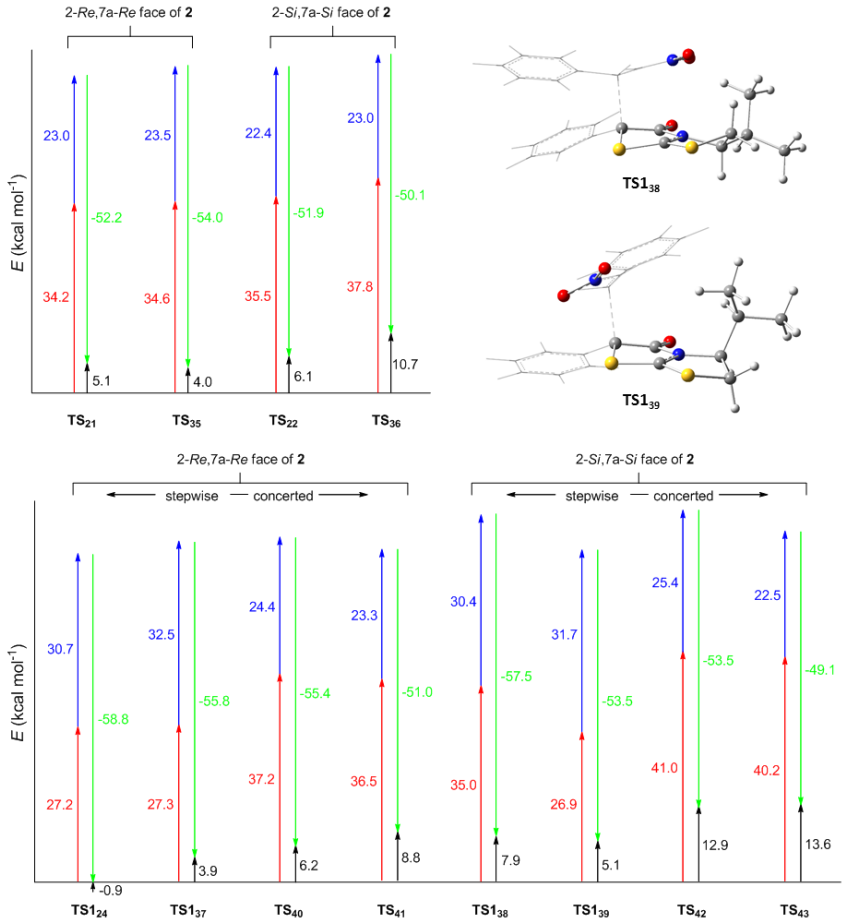

Figure 21. Distortion energies of the dipole (red) dipolarophiles (blue), interaction energies (green) and activation energies (black) for the reactions of chiral thioisomünchnone **2** with dipolarophiles **3** (above) and **5** (below) along with optimized structures of the saddle points **TS1$_{38}$** and **TS1$_{39}$** at the M06-2X/6-311++G(d,p) level in CH_2Cl_2 (SMD method). For clarity the backbone of the dipole and the nitro group has been represented with balls, whereas the remaining molecular fragments are depicted with wireframe.

Journal Name

ARTICLE

The distortion energy of the dipole for the reaction with (*E*)-(2-nitrovinyl)benzene (**5**) also matches the free energy barriers obtained (Figures 19 and 20). The saddle points corresponding to the concerted cycloadditions show that the approach of **5** to the 2-*Si*,7a-*Si* face of **2** (**TS$_{42}$** and **TS$_{43}$**) gives rise to higher values of $\Delta G^{\ddagger}$ and distortion energy of the dipole than the approach of **5** to the 2-*Re*,7a-*Re* face of **2** (**TS$_{40}$** and **TS$_{41}$**). On the other hand, the results obtained for the stepwise processes agree with those of the reaction with 1-phenyl-1*H*-pyrrole-2,5-dione (**3**), where the *exo* approach of the dipolarophile to the 2-*Si*,7a-*Si* face of **2** (**TS1$_{39}$**) leads to a similar distortion energy than that of the approach to the opposite face (2-*Re*,7a-*Re*) (**TS1$_{24}$** and **TS1$_{37}$**). These differences in the distortion energy of the dipole for **TS1$_{38}$** and **TS1$_{39}$** can be visualized in Figure 21, where the *endo* approach of **5** to **2** in **TS1$_{38}$** forces the dipole to distort due to the proximity of both isopropyl and nitro groups.

We have noted previously that the reaction of thioisomünchnone **1** led to a thioether derivative (**18**) when reacted with but-3-en-2-one (**7**)**.** This behavior could also be detected in the reaction between the chiral dipole **2** and (*E*)-(2-nitrovinyl)benzene (**5**), where the enantiomerically pure thioether **25** comes, unequivocally, from the *endo* cycloadduct (**24**). Compound **25** could then be generated by conjugate addition of thiolate **45** or thiol **26** to one additional molecule of **5**. The intermediacy of **26** would require the abstraction of H-8 by the sulfur atom attached to C-6 in **45** (Scheme 1). Cycloadduct **14** could evolve in a similar way, although compound **46** was not detected experimentally.

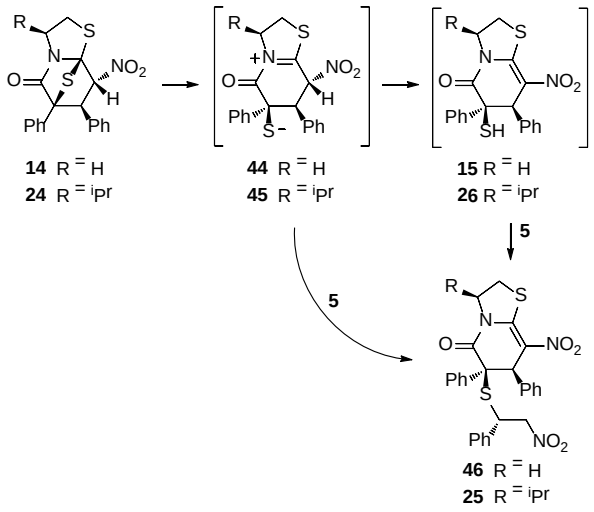

Scheme 1. Possible transformations of cycloadducts **14** and **24** to yield thiols **15** and **26** or thioethers **46** and **25**.

Figure 22 shows the reaction pathways for the formation of thiols **15** and **26** from cycloadducts **14** and **24**, respectively. The conjugate addition of the second unit of (*E*)-(2-nitrovinyl)benzene (**5**) could take place either by reaction of thiols **15** and **26** or thiolates **44** and **45**. The markedly higher stability of thiols relative to that of thiolates [even isolable in one case (**15**)], and the fact that **44** and **45** must be stronger nucleophiles, suggests that the formation of **15** and **26** would take place through the intermediacy of **44** and **45**. The reaction profiles depicted in Figure 22 show that, even though the energy barriers involved in the formation of **15** and **26** are identical, the rate-limiting step and the relative stability of the zwitterionic intermediates **44** and **45** is different. Accordingly, if these intermediates were formed, the average life of **45** should be higher than that of **44**, which would account for the subsequent reaction of **45** with another molecule of (*E*)-(2-nitrovinyl)benzene to give the cycloadduct **25**.

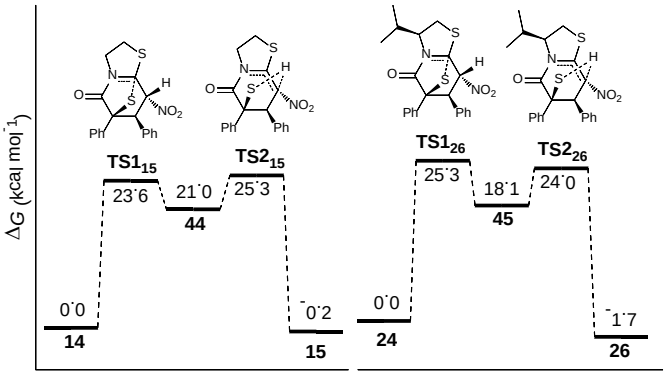

Figure 22. Relative free energy values (ΔG, kcal mol^{-1}) of all stationary points involved in the transformation of **14** and **24** into thiols **15** and **26**, respectively, calculated at the M06-2X/6-311++G(d,p) level in CH_2Cl_2 (SMD method).

Conclusions

The reactivity of 2-phenyl-5,6-dihydrothiazolo[2,3-b]thiazol-4-ium-3-olate (**1**) against symmetrical [1-phenyl-1*H*-pyrrole-2,5-dione (**3**) and dimethyl maleate (**4**)] and asymmetrical [(*E*)-(2-nitrovinyl)benzene (**5**), acrylonitrile (**6**), and but-3-en-2-one (**7**)] olefinic dipolarophiles, as well as the unichiral version (**2**) with **3** and **5** have been investigated in detail. The cycloaddition of **1** with 1-phenyl-1*H*-pyrrole-2,5-dione (**3**) was not diastereoselective, which contrasts to the situation with dimethyl maleate (**4**), from which only the *exo* cycloadduct (**11**) could be obtained. The reactions with unsymmetrically-substituted dipolarophiles (**5**-**7**) were found to be completely regioselective. The isopropyl group of the unichiral

thioisomünchnone **2** dictates a marked facial stereocontrol against bulky dipolarophiles like **3** and **5**, giving rise to enantiomerically-pure cycloadducts. Computational results at the M062-X/6-311++G(d,p) level with inclusion of solvent effects (SMD model) have demonstrated that these kinetically-controlled 1,3-dipolar cycloadditions are concerted transformations of varied synchronicity with the sole exception of (*E*)-(2-nitrovinyl)benzene (**5**), which takes place by a stepwise mechanism with the characterization of zwitterionic intermediates that evolve to the most favored regioisomers. A natural bond orbital (NBO) analysis of molecular interactions at the saddle points reveals that cycloadditions with symmetrical dipolarophiles are favored when back-donation (electron flux from dipolarophile to dipole) overcomes the donation effect. On the contrary, when this situation occurs with asymmetrical dipolarophiles, the resulting cycloadditions are disfavored, i.e. such saddle points lead to the non-observed regioisomers. However, the transition structures evolving into the favored regioisomers exhibit strong donation processes. Analyses of the energy barriers for unichiral thioisomünchnone **2** show in general a pronounced facial stereoselection, which agrees with the distortion energy of the dipole.

Experimental section

General methods. Solvents and reagents were purchased from commercial suppliers and used without further purification. The identity of all compounds was confirmed by their elemental analyses, melting points, NMR and crystallographic data (Electronic Supplementary Information). Optical rotations were measured using a Na lamp ($[\alpha]_D$ values at λ = 589 nm).

Computational details. All the geometries were optimized by the density functional theory (DFT) with the M06-2X[18] in combination with 6-311++G(d,p)[19] basis set and were performed with Gaussian09 program package[20]. The geometries were optimized including solvation effects in toluene and dichloromethane, which have been estimated by the well-established solvation model density (SMD)[21] method that takes into account different contributions such as long-range electrostatic polarization (bulk solvent effect). The IRC analysis (intrinsic reaction coordinate) for the cycloadditions involving compound **1** demonstrate that each saddle point belongs to the reaction path. Ground and transition structures were characterized by none and one imaginary frequency, respectively. All the relative energies shown are free energies calculated at 298.15 K with respect to the reagents. The orbital interaction in the saddle points and the geometries of the low-gradient region in caldera-type areas were carried out with the NBO 6.0 package[22] and visualized with Jmol.[23]

Synthetic methods.

6,8-Diphenyldihydro-2*H*-6,9*b*-epithiopyrrolo[3,4-*c*]thiazolo[3,2-*a*]pyridine-5,7,9(3*H*,8*H*,9*aH*)-trione (9). A mixture of **1** (7 mmol) and **3** (10.5 mmol) in CH_2Cl_2 (80 mL) was kept at room temperature for 24 h until the disappearance of the orange color of the mesoionic heterocycle (**1**). The solution was concentrated at reduced pressure (rotary evaporator) affording crystals of the *exo* cycloadduct (**9**) (28%). Mp 220-221 ºC; IR (KBr) ν_{max} 3060, 2934, 2358, 1707, 1497, 1445, 1380, 1260, 1186, 752, 695 cm^{-1}; ^1H NMR ($CDCl_3$, 500 MHz): δ 7.43-7.21 (m, 10H), 4.20-4.17 (m, 1H), 4.08 (d, *J* = 7.0 Hz, 1H), 3.88 (d, *J* = 7.0 Hz, 1H), 3.50-3.39 (m, 2H), 3.29-3.23 (m, 1H) ppm; ^{13}C NMR ($CDCl_3$, 125 MHz): δ 172.1, 171.5, 170.9, 131.3, 130.2, 129.1, 129.0, 128.9, 128.6, 128.3, 126.2, 87.2, 75.0, 60.0, 51.3, 46.5, 33.5 ppm. Anal. Calcd for $C_{21}H_{16}N_2O_3S_2$: C, 61.75; H, 3.95; N, 6.86; S, 15.70. Found: C, 61.57; H, 3.98; N, 6.72; S, 15.83.

6,8-Diphenyldihydro-2*H*-6,9*b*-epithiopyrrolo[3,4-*c*]thiazolo[3,2-*a*]pyridine-5,7,9(3*H*,8*H*,9*aH*)-trione (8). After filtration of compound **9**, the resulting solution was evaporated to dryness under reduced pressure to give a solid residue, which consisted of a mixture of **8** and **9**. That solid was recrystallized from ethyl acetate yielding the *endo* cycloadduct (**8**) (43%). Mp 227-229 ºC; IR (KBr) ν_{max} 3058, 2973, 2929, 2879, 1778, 1714, 1493, 1378, 1333, 1213, 1187, 760, 730, 691 cm^{-1}; ^1H NMR ($CDCl_3$, 500 MHz): δ 7,77 (d, *J* = 7.0 Hz, 2H), 7.44-7.37 (m, 6H), 7.16 (d, *J* = 7.0 Hz, 2H), 4.56 (d, *J* = 8.5 Hz, 1H), 4.30 (d, *J* = 8.5 Hz, 2H), 4.20-4.17 (m, 1H), 3.47-3.34 (m, 3H) ppm; ^{13}C NMR ($CDCl_3$, 125 MHz): δ 170.8, 170.3, 169.7, 131.3, 131.1, 129.2, 129.2, 129.1, 129.04, 128.4, 126.4, 86.2, 72.9, 59.0, 54.1, 46.6, 34.1 ppm. Anal. Calcd for $C_{21}H_{16}N_2O_3S_2$: C, 61.75; H, 3.95; N, 6.86; S, 15.70. Found: C, 61.63; H, 4.01; N, 6.80; S, 15.91.

6,8-Diphenyl-2,3-dihydropyrrolo[3,4-*c*]thiazolo[3,2-*a*]pyridine-5,7,9(8*H*)-trione (10). A mixture of cycloadducts **8** and **9** (0.5 g) in toluene (300 mL) containing silica gel [Merck 60 (400-230 mesh)] (3 g) was stirred at reflux for 72 h until the disappearance of both cycloadducts (TLC analysis: ethyl acetate:hexane 1:2 v/v). The silica gel was removed by filtration and washed with acetone until formation of a colorless solution. The solvent was removed under reduced pressure giving a solid, which was suspended in ethyl acetate yielding solid thiazolopyridone **10** that was further recrystallized from ethyl acetate (54%). Mp 195-196 ºC; IR (KBr) ν_{max} 3023, 1754, 1709, 1654, 1586, 1363, 1137, 1098, 766, 690 cm^{-1}; ^1H NMR ($CDCl_3$, 500 MHz): δ 7.50-7.34 (m, 10H), 4.48 (t, *J* = 8.0 Hz, 2H), 3.49 (t, *J* = 8.0 Hz, 2H) ppm; ^{13}C NMR ($CDCl_3$, 125 MHz): δ 164.0, 163.7, 161.7, 149.4, 134.3, 131.1, 130.0, 129.6, 128.8, 128.6, 127.8, 127.3, 126.5, 126.0, 101.6, 50.4, 28.6 ppm. Anal. Calcd for $C_{21}H_{14}N_2O_3S$: C, 67.37, H, 3.77; N, 7.48; S, 8.56. Found: C, 67.24; H, 3.81; N, 7.40; S, 8.70.

Dimethyl 5-oxo-6-phenylhexahydro-6,8*a*-epithiothiazolo[3,2-*a*]pyridine-7,8-dicarboxylate (11). A mixture of **1** (2.6 mmol) and **4** (3.8 mmol) in toluene (50 mL) was stirred at reflux during 4 h until the disappearance of the orange color of the mesoionic heterocycle (**1**). The solution was allowed to cool at room temperature, affording crystals of the *exo* cycloadduct **11** (71%). Mp 185-187 ºC; IR (KBr) ν_{max} 3452, 3406, 3034, 2946, 2880, 2835, 2361, 1742, 1716, 1447, 1354, 1217,

1159, 1058, 965, 949, 844, 748, 697; cm^{-1}; ^1H NMR ($CDCl_3$, 500 MHz): δ 7.36-7.27 (m, 5H), 4.19-4.16 (m, 1H), 4.11 (d, 1H, *J* = 9.0 Hz), 3.74 (d, 1H, *J* = 9.0 Hz), 3.69 (s, 3H), 3.36-3.33 (m, 2H), 3.24 (s, 3H), 3.12-3.08 (m, 1H). ^{13}C NMR ($CDCl_3$, 125 MHz): δ 171.6, 169.7, 168.6, 131.1, 128.7, 128.3, 128.1, 86.0, 74.1, 63.0, 55.2, 52.3, 51.8, 45.7, 32.9 ppm. Anal. Calcd for $C_{17}H_{17}NO_5S_2$: C, 53.81; H, 4.52; N, 3.69; S, 16.90. Found: C, 53.78; H, 4.49; N, 3.71; S, 17.15.

8-Nitro-6,7-diphenyltetrahydro-6,8*a*-epithiothiazolo[3,2-*a*]pyridin-5(6*H*)-one (14). A mixture of **1** (2.12 mmol) and (*E*)-(2-nitrovinyl)benzene (**5**) (3.21 mmol) in CH_2Cl_2 (25 mL) was kept at room temperature for 72 h until the disappearance of the orange color of the mesoionic heterocycle (**1**). The solvent was evaporated to dryness affording a solid residue that was treated with ethyl acetate yielding the title compound, which could be obtained in pure form by recrystallization from ethyl acetate (63%). Mp 204-205 ºC; IR (KBr) ν_{max} 3414, 3064, 3036, 2994, 2934, 2881, 1719, 1550, 1366, 1332, 939, 860, 775, 741, 702, 694, 609 cm^{-1}; ^1H NMR ($CDCl_3$, 500 MHz): δ 7.28-7.30 (m, 2H), 7.03-7.12 (m, 6H), 7.03-7.05 (m, 2H), 5.78 (d, *J* = 4.5 Hz, 1H), 4.54 (d, *J* = 5.0 Hz, 1H), 4.25 (m, 1H), 3.47 (m, 2H), 3.29 (m, 1H) ppm; ^{13}C NMR ($CDCl_3$, 125 MHz): δ 171.1, 135.7, 131.0, 128.5, 128.4, 128.4, 128.3, 128.2, 128.0, 97.8, 86.1, 77.2, 56.0, 46.2, 33.9. Anal. Calcd for $C_{19}H_{16}N_2O_3S_2$: C, 59.35, H, 4.19; N, 7.29; S, 16.68. Found: C, 59.22; H, 4.18; N, 7.25; S, 16.79.

6-Mercapto-8-nitro-6,7-diphenyl-6,7-dihydro-2*H*-thiazolo[3,2-*a*]pyridin-5(3*H*)-one (15). To a solution of compound **14** (0.2 g) in CH_2Cl_2 (30 mL) was added silica gel [Merck 60 (400-230 mesh)] (3 g) and the mixture was stirred at reflux for 19 h until the disappearance of **14** (TLC analysis: ethyl acetate:hexane 1:2 v/v). The silica gel was removed by filtration and washed with dichloromethane until a colorless solution resulted. The solvent was removed under reduced pressure giving rise to thiol **15**, which was crystallized from diethyl ether on standing (52%). Mp 213-214 ºC; IR (KBr) ν_{max} 3059, 2941, 2892, 2558, 1695, 1578, 1446, 1300,1234, 1186, 721, 697 cm^{-1}; ^1H NMR ($CDCl_3$, 500 MHz): δ 7.33-7.43 (m, 8H), 7.22-7.24 (m, 2H), 5.33 (s, 1H), 4.70-4.75 (m, 1H), 4.14-4.20 (m, 1H), 3.15-3.25 (m, 2H), 2.33 (s, 1H) ppm; ^{13}C NMR ($CDCl_3$, 125 MHz): δ 168.1, 154.7, 139.3, 135.8, 129.4, 129.1, 129.0, 128.8, 128.7, 126.9, 125.3, 60.0, 50.5, 50.1, 28.6. Anal. Calcd for $C_{19}H_{16}N_2O_3S_2$: C, 59.35, H, 4.19; N, 7.29; S, 16.68. Found: C, 59.27; H, 4.15; N, 7.28; S, 16.80.

5-Oxo-6-phenylhexahydro-6,8*a*-epithiothiazolo[3,2-*a*]pyridine-8-carbonitrile (16). Compound **1** (2.98 mmol) was dissolved in acrylonitrile (**6**) (20 mL) and kept at room temperature for 24 h until the disappearance of the orange color of **1**. The *endo* cycloadduct **16** was isolated by column chromatographic (ethyl acetate:petroleum ether 1:5 v/v) and recrystallized from ethyl acetate (18%). Mp 134-135 ºC; IR (KBr) ν_{max} 3422, 3058, 3031, 2826, 2874, 2237, 1717, 1598, 1445, 1360, 1332, 1261, 1185, 1112, 978, 927, 794, 765, 708 697, 673, 574, 501, 457 cm^{-1}; ^1H NMR ($CDCl_3$, 500 MHz): δ 7.45-7.36 (m, 5H), 4.20-4.16 (m, 1H), 3.97-3.95 (dd, 1H, *J* = 4 Hz, *J* = 10 Hz), 3.71-3.65 (m, 1H), 3.51-3.43 (m, 2H), 3.21-3.17 (dd, 1H, *J* = 10 Hz, *J* = 13 Hz), 3.05-3.01 (dd, 1H, *J* = 4 Hz, *J* = 13 Hz). ppm; ^{13}C NMR ($CDCl_3$, 125 MHz): 171.7, 132.8, 129.0, 128.7, 127.9, 117.9, 87.1, 71.4, 46.4, 44.5, 40.9, 34.5. Calcd for $C_{14}H_{12}N_2OS_2$: C, 58.31; H, 4.19; N, 9.71; S, 22.24. Found: C, 58.27; H, 4.21; N, 9.68; S, 22.07.

5-Oxo-6-phenylhexahydro-6,8*a*-epithiothiazolo[3,2-*a*]pyridine-8-carbonitrile (17). In following the same methodology as for *endo* cycloadduct **16**, the *exo* cycloadduct was recrystallized from ethyl acetate. (20%). Mp 157-158 ºC; IR (KBr) ν_{max} 3409, 3059, 2936, 2884, 2243, 1800, 1718, 1595, 1444, 1363, 1299, 1218, 1151, 1070, 989, 938, 844, 702, 626, 558, 491 cm^{-1}; ^1H NMR ($CDCl_3$, 500 MHz): δ 7.45-7.38 (m, 5H), 4.18-4.11 (m, 1H), 3.57-3.55 (dd, 1H, *J* = 3.5 Hz, *J* = 8 Hz), 3.51-3.43 (m, 2H), 3.34-3.29 (m, 1H), 3.18-3.14 (dd, 1H, *J* = 8 Hz, *J* = 13 Hz), 3.03-3.00 (dd, 1H, *J* = 4 Hz, *J* = 13 Hz). ppm; ^{13}C NMR ($CDCl_3$, 125 MHz): 172.0, 132.6, 129.0, 128.7, 128.0, 118.9, 88.3, 71.3, 46.1, 45.8, 41.5, 34.2. Calcd for $C_{14}H_{12}N_2OS_2$: C, 58.31; H, 4.19; N, 9.71; S, 22.24. Found: C, 58.25; H, 4.22; N, 9.69; S, 22.10.

8-Acetyl-6-((3-oxobutyl)thio)-6-phenyl-6,7-dihydro-2H-thiazolo[3,2-*a*]pyridin-5(3*H*)-one (18). Compound **1** (4.26 mmol) was dissolved in but-3-en-2-one (**7**) (20 mL) and heated at reflux for 30 minutes, until the disappearance of the orange color of **1**. The solution was evaporated to dryness and the residue was dissolved in warm ethyl acetate. After cooling to room temperature the tittle compound crystallized as a white solid (32%). Mp 182-183 ºC; IR (KBr) ν_{max} 3338, 2980, 2879, 2829, 1705, 1678, 1639, 1518, 1372, 1248, 1202, 1125, 985, 849, 706, 588, 461 cm^{-1}; ^1H NMR ($CDCl_3$, 500 MHz): δ 7.54-7.53 (d, 2H, *J* = 7.5 Hz), 7.40-7.37 (t, 2H, *J* = 7.5 Hz), 7.32-7.29 (t, 1H, *J* = 7.5 Hz), 4.26-4.23 (t, 2H, *J* = 7.5 Hz), 3.24-3.20 (d, 1H, *J* = 16.5 Hz), 3.19-3.10 (m, 2H), 3.05-3.02 (d, 1H, *J* = 16.5 Hz), 2.66-2.63 (t, 2H, *J* = 6.5 Hz), 2.56-2.53 (t, 2H, *J* = 6.5 Hz), 2.21 (s, 3H), 2.07 (s, 3H). ppm; ^{13}C NMR ($CDCl_3$, 125 MHz): 205.9, 193.5, 167.0, 151.8, 138.3, 128.5, 127.8, 127.5, 105.7, 56.9, 47.9, 42.3, 39.2, 29.7, 28.0, 27.1, 23.9. Anal. Calcd for $C_{19}H_{21}NO_3S_2$: C, 60.77; H, 5.64; N, 3.73; S, 17.08. Found: C, 60.62; H, 5.72; N, 3.65; S, 16.78.

8-Acetyl-6-phenyltetrahydro-6,8*a*-epithiothiazolo[3,2-*a*]pyridin-5(6*H*)-one (20). From the reaction mixture of **1** and **7**, the *exo* cycloadduct **20** could be isolated by column chromatography (ethyl acetate:petroleum ether 1:5 v/v). Recrystallized from ethyl acetate (22%) had mp 178-179 ºC; IR (KBr) ν_{max} 3344, 3083, 2943, 2889, 1686, 1640, 1442, 1374, 1347, 1115, 950, 925, 842, 749, 628 cm^{-1}; ^1H NMR ($CDCl_3$, 500 MHz): δ 7.45-7.43 (dd, 2H, *J* = 1.5 Hz y *J* = 8.5 Hz), 7.34-7.29 (m, 3H), 5.00-4.98 (dd, 1H, *J* = 2.5 Hz, *J* = 6.5 Hz), 4.28-4.21 (m, 1H), 4.05-3.99 (m, 1H), 3.52-3.48 (dd, 1H, *J* = 2.5Hz, *J* = 16.5 Hz), 3.16-3.09 (m, 2H), 3.03-2.99 (m, 1H), 2,29 (s, 3H) ppm; ^{13}C NMR ($CDCl_3$, 125 MHz): 194.84, 166.02, 135.69, 134.65, 128.66, 128.51, 127.35, 94.59, 59.78, 48.57, 33.86, 30.13, 28,26. Anal. Calcd for $C_{15}H_{15}NO_2S_2$: C, 58.99, H, 4.95; N, 4.59; S, 21.00. Found: C, 58.73; H, 5,11; N, 4.48; S, 19.85.

(3*S*,6*S*,6a*S*,9a*R*,9b*S*)-3-Isopropyl-6,8-diphenyldihydro-2*H*-6,9*b*-epithiopyrrolo[3,4-*c*]thiazolo[3,2-*a*]pyridine-5,7,9(3*H*,8*H*,9a*H*)-trione (21). A mixture of **2** (2.2 mmol) and **3** (3.3 mmol) in CH_2Cl_2 (80 mL) was kept at room temperature for 24 h until the disappearance of the orange color of the mesoionic heterocycle (**2**). The solvent was evaporated to

dryness under reduced pressure and the resulting residue was dissolved in ethyl acetate. Further addition of petroleum ether (6 mL) resulted in crystals of the title compound (72%). Mp 221-223 ºC; $[\alpha]_D$ 52.3º (c 4.6 CH_2Cl_2); IR (KBr) ν_{max} 3477, 3063, 3034, 2962, 2873, 1781, 1704, 1596, 1498, 1375, 1195, 751, 694 cm^{-1}; ^1H NMR ($CDCl_3$, 500 MHz): δ 7.35-7.44 (m, 8H), 7.20-7.23 (m, 2H) 4.02 (d, *J* = 7 Hz, 1H), 3.98-4.00 (m, 1H), 3.84 (d, *J* = 7 Hz, 1H), 3.36 (dd, *J* = 8.5 Hz, *J* = 11.5 Hz, 1H), 3.24 (q, 1H, *J* = 5.5 Hz), 2.94-3.01 (m, 1H), 1.01 (d, *J* = 7.5 Hz, 1H), 0.91 (d, *J* = 6.5 Hz, 3H) ppm; ^{13}C NMR ($CDCl_3$, 125 MHz): δ 171.9, 171.0, 169.9, 131.4, 130.6, 129.10, 129.0, 128.9, 128.7, 128.2, 126.2, 88.0, 66.2, 60.6, 50.6, 33.5, 26.6, 20.2, 16.1. Anal. Calcd for $C_{24}H_{22}N_2O_3S_2$: C, 63.98, H, 4.92; N, 6.22; S, 14.23. Found: C, 63.87; H, 4.90; N, 6.18; S, 14.40.

(3*S*,6*R*,6*aR*,9*aS*,9*bR*)-3-Isopropyl-6,8-diphenyldihydro-2*H*-6,9*b*-epithiopyrrolo[3,4-*c*]thiazolo[3,2-*a*]pyridine-5,7,9(3*H*,8*H*,9*aH*)-trione (22). After filtration of compound **21**, the resulting solution was evaporated to dryness under reduced pressure giving a solid that was dissolved in diethyl ether, crystallizing subsequently a mixture of cycloadduct **22** and **2**. Further recrystallization from diethyl ether afforded pure **22** (15%). Mp 223-224 ºC; $[\alpha]_D$ 18.7º (c 5.2 CH_2Cl_2); IR (KBr) ν_{max} 3476, 3065, 3033, 2967, 2936, 2901, 2872, 1781, 1713, 1596, 1495, 1388, 1189, 772, 753, 694 cm^{-1}; ^1H NMR ($CDCl_3$, 500 MHz): δ 7.34-7.43 (m, 8H), 7.21-7.23 (m, 2H) 4.12 (d, *J* = 7 Hz, 1H), 3.96 (dd, *J* = 6.0 Hz, *J* = 9.5 Hz, 1H), 3.87 (d, *J* = 6.5 Hz, 1H), 3.50 (q, *J* = 6.0 Hz, 1H), 3.18 (d, *J* = 12.0 Hz, 1H), 2.00-2.10 (m, 1H), 1.03 (d, *J* = 6.5 Hz, 3H), 0.97 (d, *J* = 6.5 Hz, 3H) ppm. ^{13}C NMR ($CDCl_3$, 125 MHz): δ 172.3, 172.1, 170.8, 131.4, 130.4, 129.1, 129.0, 128.9, 128.7, 128.3, 126.2, 87.5, 74.6, 65.3, 60.3, 51.3, 36.0, 31.1, 19.9, 19.7. Anal. Calcd for $C_{24}H_{22}N_2O_3S_2$: C, 63.98, H, 4.92; N, 6.22; S, 14.23. Found: C, 63.90; H, 4.94; N, 6.20; S, 14.37.

(*S*)-3-Isopropyl-6,8-diphenyl-2,3-dihydropyrrolo[3,4-*c*]thiazolo[3,2-*a*]pyridine-5,7,9(8*H*)-trione (23). In following the same procedure as for **10**, the title compound was isolated after reaction completion (48 h). Recrystallization from diethyl ether gave the pure compound in 37% yield. Mp 222-223 ºC; $[\alpha]_D$ 255.7º (c 5.4 CH_2Cl_2); IR (KBr) ν_{max} 3454, 3060, 3022, 2965, 2929, 2880, 1758, 1713, 1642, 1371, 1111, 767, 693, 620 cm^{-1}; ^1H NMR ($CDCl_3$, 500 MHz): δ 7.50-7.52 (m, 2H), 7.35-7.45 (m, 8H) 5.12-5.15 (m, 1H), 3.65 (dd, J_1 = 9.0 Hz, J_2 = 11.5 Hz, 1H), 3.40 (dd, *J* = 1.5 Hz, *J* = 11.5 Hz, 1H), 2.63-2.70 (m, 1H), 1.10 (d, *J* = 7.0 Hz, 3H), 0.99 (d, *J* = 7.0 Hz, 3H) ppm; ^{13}C NMR ($CDCl_3$, 125 MHz): δ 164.4, 164.2, 162.0, 150.2, 134.5, 131.6, 130.5, 130.1, 129.1, 128.9, 128.1, 127.6, 126.9, 126.3, 101.5, 68.0, 29.5, 29.2, 19.4, 16.2. Anal. Calcd for $C_{24}H_{20}N_2O_3S$: C, 69.21, H, 4.84; N, 6.73; S, 7.70. Found: C, 69.39; H, 4.90; N, 6.49; S, 7.89.

(3*S*,6*S*,7*R*,8*R*,8*aS*)-3-Isopropyl-8-nitro-6,7-diphenyltetrahydro-6,8*a*-epithiothiazolo[3,2-*a*]pyridin-5(6*H*)-one (24). A mixture of **2** (3.6 mmol) and **5** (4 mmol) in CH_2Cl_2 (45 mL) was kept at room temperature for 30 h, the solvent was removed under reduced pressure, and the resulting crude was suspended in diethyl ether yielding compound **24**, which was recrystallized from diethyl ether (78%). Mp 137-139 ºC; $[\alpha]_D$ 382.6º (c 5.2 CH_2Cl_2); IR (KBr) ν_{max} 3399, 3060, 3032, 3009, 2960, 2896, 2873, 1709, 1555, 1374, 1361, 1324, 1276, 697 cm^{-1}; ^1H NMR ($CDCl_3$, 500 MHz): δ 7.26-7.30 (m, 2H), 7.10-7.20 (m, 8H) 5.70 (d, *J* = 4.5 Hz, 1H), 4.44 (d, *J* = 4.5 Hz, 1H), 4.14-4.17 (m, 1H), 3.35 (dd, *J* = 7.0 Hz, *J* = 11 Hz, 1H), 3.26 (dd, *J* = 5.5 Hz, *J* = 11.5 Hz, 1H) 2.92-2.96 (m, 1H), 0.98 (dd, *J* = 2.0 Hz, *J* = 7.0 Hz, 6H) ppm; ^{13}C NMR ($CDCl_3$, 125 MHz): δ 169.6, 135.6, 131.2, 128.5, 128.3, 128.2, 127.9, 100.2, 87.0, 78.9, 65.1, 55.9, 34.0, 27.4, 19.8, 15.9. Anal. Calcd for $C_{22}H_{22}N_2O_3S_2$: C, 61.95, H, 5.20; N, 6.57; S, 15.03. Found: C, 61.85; H, 5.22; N, 6.43; S, 15.28.

(3*S*,6*S*,7*R*,8*R*)-3-Isopropyl-8-nitro-6-((*R*)-2-nitro-1-phenylethyl)thio)-6,7-diphenyltetrahydro-2*H*-thiazolo[3,2-*a*]pyridin-5(3H)-one (25). In following the same procedure as for **24**, although using a different molar ratio of the starting materials, 1:1.5 (**2**:**5**), the title compound was isolated after reaction completion (48 h). The solvent was evaporated under reduced pressure, and further addition of diethyl ether resulted in crystals of compound **24** in 33% yield. The filtrate was evaporated under reduced pressure and the crude was dissolved in methanol crystallizing **25** in 22% yield. Mp 189-191 ºC; $[\alpha]_D$ 26.7º (c 5.1 CH_2Cl_2); IR (KBr) ν_{max} 3407, 3060, 3030, 2967, 1705, 1581, 1551, 1455, 1376, 1311, 1215, 1191, 696 cm^{-1}; ^1H NMR ($CDCl_3$, 500 MHz): δ 7.51 (d, *J* = 7.5 Hz, 2H), 7.44 (t, *J* = 7.5 Hz,2H), 7.35-7.40 (m, 3H), 7.27-7.30 (m, 3H), 7.14-7.22 (m, 5H), 5.47 (s, 1H), 5.04-5.10 (m, 1H), 4.60 (dd, *J* = 4.5 Hz, *J* = 11.5 Hz, 1H), 4.30 (dd, *J* = 11.5 Hz, *J* = 13.0 Hz, 1H), 3.25 (dd, *J* = 8.5 Hz, *J* = 12.0 Hz, 1H), 3.16 (dd, *J* = 4.5 Hz, *J* = 13.0 Hz, 1H), 3.05 (dd, *J* = 1.0 Hz, *J* = 12.0 Hz, 1H), 2.60-2.64 (m, 1H), 1.1 (d, *J* = 6.5 Hz, 3H), 1.00 (d, *J* = 7.0 Hz, 3H) ppm; ^{13}C NMR ($CDCl_3$, 125 MHz): δ 168.3, 155.7, 137.2, 136.6, 134.5, 129.9, 129.6, 128.9, 128.8, 128.1, 127.5, 126.5, 126.2, 78.1, 67.7, 63.2, 49.0, 45.6, 30.8, 29.2, 19.8, 17.0. Anal. Calcd for $C_{30}H_{29}N_3O_5S_2$: C, 62.59, H, 5.08; N, 7.30; S, 11.14. Found: C, 62.42; H, 5.03; N, 7.21; S, 11.30.

Transformation of 24 into 25 catalyzed by silica gel. A mixture of **24** (1.95 mmol) and silica gel (10 g) in CH_2Cl_2 (100 mL) was heated at reflux for 72 h. TLC monitoring (ethyl acetate:hexane 1:3 v/v) revealed that the initial cycloadduct did not disappear completely. The catalyst was removed by filtration and washed with CH_2Cl_2 until formation of a colorless solution. The solvent was removed under reduced pressure giving a solid residue, which was suspended in diethyl ether and led to compound **25** (5%).

Transformation of 24 into 25 in the presence of (*E*)-(2-nitrovinyl)benzene (5). A solution of cycloadduct **24** and (*E*)-(2-nitrovinyl)benzene (**5**) in CH_2Cl_2 (molar ratio 1:1) was stirred for five days. TLC analysis (ethyl acetate:hexane 1:3 v/v) showed the formation of a new compound, which was purified by preparative TLC and had spectroscopic data identical to a pure sample of **25**.

Conflicts of interest

There are no conflicts to declare.

Acknowledgements

We thank the financial support from the *Junta de Extremadura* and *Fondo Europeo de Desarrollo Regional* (Grants GR15022 and IB16167). Computational assistance was provided by the

supercomputer LUSITANIA, which is supported by *Cenits* and *Computaex* Foundation.

Notes and references

(1) (a) *Synthetic Applications of 1,3-Dipolar Cycloaddition Chemistry Toward Heterocycles and Natural Products*, eds. A. Padwa and W. H. Pearson, John Wiley & Sons, New York, 2002; (b) H. Pellisier, *Tetrahedron*, 2007, **63**, 3235-3285; (c) H. Suga and K. Itoh, in *Methods and Applications of Cycloaddition Reactions in Organic Syntheses*, ed. N. Nishiwaki, John Wiley & Sons, Hoboken, New Jersey, 2013, pp. 175-204; (d) T. Hasimoto and K. Maruoka, *Chem. Rev.,* 2015, **115**, 5366-5412; (e) M. S. Singh, S. Chowdhury and S. Koley, *Tetrahedron* 2016, **72**, 1603-1644.

(2) (a) J. A. Prescher and C. R. Bertozzi, *Nat. Chem. Biol.,* 2005, **1**, 13-21; (b) J. F. Lutz and Z. Zarafshani, *Drug Deliv. Res.,* 2008, **60**, 958-970; (c) R. Narayan, M. Potowski, Z. J. Jia, A. P. Antonchick and H. Waldmann, *Acc. Chem. Res.,* 2014, **47**, 1296-1310.

(3) For studies on natural dipolar cycloadditions: a) K. A. P. Payne, M. D. White, K. Fisher, B. Khara, S. S. Bailey, D. Parker, N. J. W. Rattray, D. K. Trivedi, R. Goodacre, R. Beveridge, P. Barran, S. E. J. Rigby, N. S. Scrutton, S. Hay and D. Leys, *Nature,* 2015, **522**, 497-501. b) M. D. White, K. A. P. Payne, K. Fisher, S. Marshall, D. Parker, N. J. W. Rattray, D. K. Trivedi, R. Goodacre, S. E. J. Rigby, N. S. Scrutton, S. Hay and D. Leys, *Nature,* 2015, **522**, 502-506.

(4) (a) W. Xi, T. F. Scott, C. J. Kloxin and C. N. Bowman, *Adv. Funct. Mater.*, 2014, **24**, 2572-2590; (b) G. Delaittre, N. K. Guimard and C. Barner-Kowollik, *Acc. Chem. Res.*, 2015, **48**, 1296-1307; (c) W. Yan, S. M. Seifermann, P. Pierrat and S. Brase, *Org. Biomol. Chem.*, 2015, **13**, 25-54.

(5) For classical and comprehensive reviews on mesoionic structures and reactions of mesoionic dipoles: (a) W. D. Ollis and C. A. Ramsden, in *Advances in Heterocyclic Chemistry*, eds. A. R. Katritzky and A. J. Boulton, *Academic Press*, New York, 1976, Vol. 19, pp. 1-122; (b) C. G. Newton and C. A. Ramsden, *Tetrahedron*, 1982, **38**, 2965-3011; (c) K. T. Potts, in *1,3-Dipolar Cycloaddition Chemistry*, ed. A. Padwa, John Wiley & Sons, New York, 1984, Vol. 2, pp. 1-82; (d) W. D. Ollis, S. P. Stanforth and C. A. Ramsden, *Tetrahedron*, 1985, **41**, 2239-2329; (e) M. H. Osterhout, W. R. Nadler and A. Padwa, *Synthesis*, 1994, 123-141.

(6) For recent reviews and treatments on mesoionics-based chemistry: (a) G. W. Gribble, in *Synthetic Applications of 1,3-Dipolar Cycloaddition Chemistry Toward Heterocycles and Natural Products*, eds. A. Padwa and W. H. Pearson, John Wiley & Sons, New York, 2002, pp. 681-753; (b) M. Ávalos, R. Babiano, P. Cintas, J. L. Jiménez and J. C. Palacios, *Acc. Chem. Res.,* 2005, **38**, 460-468; (c) J. M. Lopchuk, in *Metalation of Azoles and Related Five-Membered Ring Heterocycles*, ed. G. W. Gribble, Springer, Berlin, 2012, pp. 381-413.

(7) For recent and representative examples involving different mesoionic heterocycles: (a) D. L. Browne and P. A. Harrity, *Tetrahedron*, 2010, **66**, 553-568; (b) J. M. Lopchuk, R. P. Hughes and G. W. Gribble, *Org. Lett*., 2013, **15**, 5218-5221; (c) M. S. Morin, D. J. St-Cyr, B. A. Arndtsen, E. H. Krenske and K. N. Houk, *J. Am. Chem. Soc*., 2013, **135**, 17349-17358; (d) J. Marco-Martínez, S. Reboredo, M. Izquierdo, V. Marcos, J. L. López, S. Filippone and N. Martín, *J. Am. Chem. Soc*., 2014, **136**, 2897-2904; (e) S. Specklin, E. Decuypere, L. Plougastel, S. Aliani and F. Taran, *J. Org. Chem*., 2014, **79**, 7772-7777; (f) H. rguven, D. C. Leitch, E. N. Keyzer and B. A. Arndtsen, *Angew. Chem. Int. Ed.,* 2017, **56**, 6078-6082.

(8) For recent examples: (a) D. Cantillo, M. Ávalos, R. Babiano, P. Cintas, J. L. Jiménez, M. E. Light and J. C. Palacios, *Org. Lett*., 2008, **10**, 1079-1082; (b) D. Cantillo, M. Ávalos, R. Babiano, P. Cintas, J. L. Jiménez, M. E. Light and J. C. Palacios, *J. Org Chem*., 2009, **74**, 3698-3705; (c) D. Cantillo, M. Ávalos, R. Babiano, P. Cintas, J. L. Jiménez, M. E. Light and J. C. Palacios *J. Org. Chem*., 2009, **74**, 7644-7650; (d) D. Cantillo, M. Ávalos, R. Babiano, P. Cintas, J. L. Jiménez, M. E. Light, J. C. Palacios and V. Rodríguez, *Org. Biomol. Chem*., 2010, **8**, 7644-7650; (e) D. Cantillo, M. Ávalos, R. Babiano, P. Cintas, J. L. Jiménez, M. E. Light and J. C. Palacios. *J. Org. Chem*., 2014, **79**, 4201-4205.

(9) M. Ávalos, R. Babiano, A. Cabanillas, P. Cintas, M. J. Diánez, M. D. Estrada, J. L. Jiménez, A. López-Castro, J. C. Palacios and S. P. Garrido, *J. Chem. Soc. Chem. Commun.,* 1995, 2213-2214.

(10) M. Ávalos, R. Babiano, A. Cabanillas, P. Cintas, F. J. Higes, J. L. Jiménez and J. C. Palacios, *J. Org. Chem.*, 1996, **61**, 3738-3748.

(11) J. García de la Concepción, M. Ávalos, R. Babiano, P. Cintas, J. L. Jiménez, M. E. Light and J. C. Palacios, *Tetrahedron,* 2016, **72**, 4665-4670.

(12) J. García de la Concepción, M. Ávalos, R. Babiano, P. Cintas, J. L. Jiménez, M. E. Light and J. C. Palacios, *Tetrahedron*, 2017, **73**, 1551-1560.

(13) In stereochemical language, chemists often allude to "homochiral" and/or "chiral non-racemic", which may engender considerable puzzling, as neither of them denote strictly enantiomerically pure samples. The latter in particular is to be discouraged (see: E. L. Eliel and S. H. Wilen, *Stereochemistry of Organic Compounds*, John Wiley & Sons, New York, 1994, p. 5), as enantioenriched samples of varied purity lie in this terminology. The term *unichiral*, introduced by Gal, and scarcely employed so far, is a useful and clever alternative that denotes single chirality and hence enantiomerically pure. See: (a) J. Gal, *Enantiomer,* 1998, **3**, 263-273; (b) J. Gal, *Chirality,* 2011, **23**, 647-659. Unless otherwise specified, we use through this paper the terms unichiral and enantiopure as synonymous.

(14) J. P. Foster and F. J. Weinhold, *J. Am. Chem. Soc*., 1980, **102**, 7211-7218.

(15) Y.-F. Yang, P. Yu and K. N. Houk, *J. Am. Chem. Soc*., 2017, **139**, 18213-18221.

(16) E. R. Johnson, S. Keinan, P. Mori-Sanchez, J. Contreras-Garcia, A. J. Cohen and W. Yang, *J. Am. Chem. Soc.,* 2010, **132**, 6498-6506.

(17) B. Lin, P. Yu, C. Q. He and K. N. Houk, *Bioorg. Med. Chem*., 2016, **24**, 4787-4790.

(18) (a) Y. Zhao and D. G. Truhlar, *Theor. Chem. Acc*., 2008, **120**, 215-241. (b) Y. Zhao and D. G. Truhlar, *Acc. Chem. Res*., 2008, **41**, 157-167.

(19) M. P. McGrath and L. Radom, *J. Chem. Phys*., 1991, 94, 511-516.
(20) M. J. Frisch, G. W. Trucks, H. B. Schlegel, G. E. Scuseria, M. A. Robb, J. R. Cheeseman, G. Scalmani, V. Barone, B. Mennucci, G. A. Petersson, H. Nakatsuji, M. Caricato, X. Li, H. P. Hratchian, A. F. Izmaylov, J. Bloino, G. Zheng, J. L. Sonnenberg, M. Hada, M. Ehara, K. Toyota, R. Fukuda, J. Hasegawa, M. Ishida, T. Nakajima, Y. Honda, O. Kitao, H. Nakai, T. Vreven, Jr., J. A. Montgomery, J. E. Peralta, F. Ogliaro, M. Bearpark, J. J. Heyd, E. Brothers, N. K. Kudin, V. N. Staroverov, R. Kobayashi, J. Normand, K. Raghavachari, A. Rendell, J. C. Burant, S. S. Iyengar, J. Tomasi, M. Cossi, N. Rega, J. M. Millam, M. Klene, J. E. Knox, J. B. Cross, V. Bakken, C. Adamo, J. Jaramillo, R. Gomperts, R. E. Stratmann, O. Yazyev, A. J. Austin, R. Cammi, C. Pomelli, J. W. Ochterski, R. L. Martin, K. Morokuma, V. G. Zakrzewski, G. A. Voth, P. Salvador, J. J. Dannenberg, S. Dapprich, A. D. Daniels, Ö Farkas, J.B. Foresman, J. V. Ortiz, J. Cioslowski and D. J. Fox, Gaussian 09, Revision D.01; Gaussian, Inc.: Wallingford, CT, 2009.
(21) A. V. Marenich, C. J. Cramer and D. G. Truhlar, *J. Phys. Chem. B*, 2009, **113**, 6378-6396.
(22) E. D. Glendening, J. K. Badenhoop, A. E. Reed, J. E. Carpenter, J. A. Bohmann, C. M. Morales, C. R. Landis, and F. Weinhold, Theoretical Chemistry Institute, University of Wisconsin, Madison, 2013.
(23) http://www.jmol.org/

